~~RL-862~~

~~RL-979~~
RL 983

DERIVATION AND APPLICATION OF A CLASS OF GENERALIZED BOUNDARY CONDITIONS - II

J. L. Volakis, T. B. A. Senior, and J.-M. Jin
The Radiation Laboratory
Department of Electrical Engineering and Computer Science
The University of Michigan
Ann Arbor, MI 48109-2122

MARCH 1989

RL-983 = RL-983

DERIVATION AND APPLICATION OF A CLASS OF GENERALIZED BOUNDARY CONDITIONS - II

J. L. Volakis, T. B. A. Senior, and J.-M. Jin
The Radiation Laboratory
Department of Electrical Engineering and Computer Science
The University of Michigan
Ann Arbor, MI 48109-2122

Abstract

Boundary conditions involving higher order derivatives are presented for simulating surfaces whose reflection coefficients are known analytically, numerically or experimentally. Procedures for determining the coefficients of the derivatives are discussed, along with the effect of displacing the surface where the boundary conditions are applied. Provided the coefficients satisfy a duality relation, equivalent forms of the boundary conditions involving tangential field components are deduced, and these provide the natural extension to non-planar surfaces. As an illustration, the simulation of metal-backed uniform and three layer dielectric coatings is given. It is shown that fourth order conditions are capable of providing an accurate simulation for the uniform coating at least a quarter of a wavelength in thickness. Provided, though, some comprise in accuracy is acceptable, it is also shown that a third order condition may be sufficient for practical purposes when simulating uniform coatings.

Table of Contents

List of Figures

I. Introduction

The use of non-metallic materials, possibly in the form of a non-uniform or multilayer coating applied to a metallic substrate, has made necessary the development of methods for simulating material effects in scattering. This is important in the analytical treatment of canonical geometries and also for the efficient generation of numerical solutions.

A possible approach is to employ approximate boundary conditions [1], and the impedance (or Leontovich) boundary condition [2] has been widely used for this purpose. But this condition allows only one degree of freedom through the single surface impedance assumed, and there are limits to the surface properties that can be simulated in this manner. The inclusion of higher order derivatives of the field components on the surface increases the flexibility, and leads to a hierarchy of boundary conditions as discussed in this paper. The first order version is equivalent to the standard impedance condition. An example of the second order version was developed by Weinstein [3] and in [4,5] to simulate thin dielectric layers with and without a metal backing. The conditions have also been used [6,7] to simulate a perfectly absorbing surface in a finite element analysis of exterior scattering problems.

In the general version considered here the boundary conditions were first employed by Karp and Karal [8] to study the surface waves supported by dielectric coatings. For a planar surface the conditions involve the normal derivatives of the normal field components, and it is shown here how they can be used to model the reflection coefficient of the surface. The required order of the condition increases with the complexity of the surface being modelled, and the effect of displacing the surface where the boundary condition is enforced is also discussed. To extend the resulting

conditions to a non-planar surface, they are first expressed in terms of the tangential components of the field, requiring the enforcement of duality. This is the same procedure used in the case of the standard (first order) impedance condition [1, 9], and it is then found that one effect of the higher order derivatives is to make the conditions less local in character through the inclusion of tangential field derivatives.

To illustrate the application of these conditions, the problem of a planar metal-backed uniform dielectric layer is examined in detail. By expanding the known reflection coefficient, boundary conditions up to the fourth order are derived. It is shown that even for a layer thickness as large as a quarter wavelength, fourth order conditions applied at the upper surface of the layer provide an excellent simulation for all angles of incidence, and their accuracy is determined. Of course, such higher order conditions are not without disadvantages, and their use in analytical and numerical work is discussed.

2. Boundary Conditions for a Planar Surface

In terms of the Cartesian coordinates x, y, z, the region $y < 0$ is occupied by a laterally homogeneous material which may, however, be stratified or have properties varying in depth. For any field incident on this medium we seek a boundary condition which can be applied at the surface $y = 0$ and will accurately reproduce the field in $y \geq 0$.

The boundary conditions proposed are

$$\prod_{m=1}^{M}\left(\frac{\partial}{\partial y}+ik\Gamma_m\right)E_y=0$$
$$\prod_{m=1}^{M'}\left(\frac{\partial}{\partial y}+ik\Gamma'_m\right)H_y=0 \qquad (1)$$

where k is the free space propagation constant and a time factor $e^{-i\omega t}$ has been assumed and suppressed. Γ_m and Γ'_m are constants which are chosen to reproduce the desired scattering properties of the surface, and since a knowledge of E_y or H_y alone is not in general sufficient to determine an electromagnetic field, the constants cannot be chosen independently of one another.

By expanding out the product factors, the boundary conditions (1) can be written in the alternative but equivalent form

$$\sum_{m=0}^{M}\frac{a_m}{(ik)^m}\frac{\partial^m}{\partial y^m}E_y=0$$
$$\sum_{m=0}^{M'}\frac{a_m'}{(ik)^m}\frac{\partial^m}{\partial y^m}H_y=0 \qquad (2)$$

where a_m and a_m' can be expressed in terms of Γ_m and Γ_m' by equating the coefficients of like derivatives. As an example, for M = M' = 3,

$$a_o=\Gamma_1\Gamma_2\Gamma_3\ , \qquad a_1=\Gamma_1\Gamma_2+\Gamma_2\Gamma_3+\Gamma_3\Gamma_1\ ,$$
$$a_2=\Gamma_1+\Gamma_2+\Gamma_3\ , \qquad a_3=1\ .$$

When $M = M' = 1$ with $\Gamma_1' = 1/\Gamma_1$, the conditions are equivalent [1] to impedance boundary conditions for a surface with normalized impedance Γ_1. They can, therefore, be regarded as generalizations of the standard impedance boundary condition that allow the simulation of a greater variety of material properties through the inclusion of additional derivative factors.

If the plane wave

$$E_y^i = e^{-ik\,(x\cos\phi + y\sin\phi)}$$

is incident on a surface $y = 0$ at which the boundary conditions (1) are imposed, the implied reflection coefficient is

$$R(\phi) = -\prod_{m=1}^{M} \frac{\Gamma_m - \sin\phi}{\Gamma_m + \sin\phi} = -\frac{\sum_{m=0}^{M} (-1)^m a_m \sin^m \phi}{\sum_{m=0}^{M} a_m \sin^m \phi} \qquad (3)$$

with an analogous expression for the reflection coefficient $R'(\phi)$ associated with the component H_y. The special case $\Gamma_m = 1$, $m = 1, 2, \ldots, M$, constitutes a model of a perfectly absorbing surface [2]. We then have

$$R(\phi) = -\tan^{2M}\left(\frac{\pi}{4} - \frac{\phi}{2}\right),$$

and as M increases, there is an increasing range of angles about $\phi = \pi/2$ (normal incidence) where R is effectively zero.

More generally, the constants Γ_m and Γ'_m can be determined from a knowledge of the actual reflection coefficient of the surface, and some possible procedures are as follows:

(i) If analytical expressions for the reflection coefficients are available, expansion in the form (3) leads immediately to the identification of Γ_m and Γ'_m.

(ii) The constants can be chosen to recover the poles of the analytical expressions, but this may produce a less accurate simulation if the reflection coefficient is not a ratio of polynomials in $\sin\phi$.

(iii) From computed or measured data for the reflection coefficients, Γ_m and Γ'_m can be obtained by curve fitting. Although this could be adequate in any given case, it would not reveal the dependence on the material parameters of the surface.

A few simple examples of a reflection coefficient $R(\phi)$ are sufficient to illustrate these procedures. In general, a plane wave reflection coefficient can be written as

$$R(\phi) = - \frac{\eta(\phi) - \sin\phi}{\eta(\phi) + \sin\phi} \qquad (4)$$

where $\eta(\phi)$ is an angle-dependent surface impedance. If $\eta = \eta_0$, independent of angle, the corresponding boundary condition has $\Gamma_1 = \eta_0$ with $\Gamma_m = 0$ for $m > 1$, and this is the standard impedance boundary condition [2]. Alternatively, if

$$\eta(\phi) = \eta_0 + \eta_1 \sin^2 \phi$$

then

$$\Gamma_{1,2} = \frac{1}{2\eta_1} \left\{ 1 \mp \sqrt{1 - 4\,\eta_0\,\eta_1} \right\}$$

with $\Gamma_m = 0$ for $m > 2$. As another example of procedure (i), if

$$\eta(\phi) = \cos\phi \quad ,$$

then for $\phi \leq \pi/4$ we can write $\eta(\phi) \approx 1 - 1/2 \sin^2 \phi$ without significant loss of accuracy, in which case $\Gamma_1 = 0.732$ and $\Gamma_2 = -2.732$ with $\Gamma_m = 0$ for $m > 2$. For $\phi \geq \pi/4$ we can set $\alpha = \pi/2 - \phi$ and use the same approximation for $\cos\alpha$. Alternatively, using procedure (ii), it is found that if $0 < \text{Re. } \phi < \pi/2$, $R(\phi)$ has a single pole at $\sin\phi = 0.707 = -\Gamma_1$. The resulting first order boundary condition is obviously not as accurate as the second order one given by procedure (i).

In addition to modelling a reflection coefficient, the generalized boundary conditions (1) allow some flexibility in the location of the surface where they are enforced. To show this, consider a surface $y = 0$ at which the reflection coefficient is $R(\phi)$. The corresponding reflection coefficient at $y = \tau$ is then $R(\phi) \exp(2ik\tau \sin\phi)$, and since

$$e^{2ik\tau\sin\phi} = \frac{1 + ik\tau\sin\phi + \frac{1}{2}(k\tau)^2\sin^2\phi + ...}{1 - ik\tau\sin\phi + \frac{1}{2}(k\tau)^2\sin^2\phi - ....} \quad , \tag{5}$$

the phase factor can be simulated using additional derivative factors in the boundary condition. In particular, if $k\tau$ is so small that terms $O\{(k\tau)^2\}$ can be neglected, one more derivative factor suffices with $\Gamma_1 = i/k\tau$, whereas to the next order in $k\tau$ two derivatives are needed with $\Gamma_{1,2} = (1 \pm i)/(ik\tau)$. This allows us to consider separately the modelling of the reflection coefficient and the phase factor, but if the location of the simulating surface is not specified a priori, it can be chosen to minimize the order of the boundary condition for a given accuracy.

3. Equivalent Forms of the Conditions

The boundary conditions (1) are scalar conditions in as much as each involves only a single field component, but in the first order case when $M = M' = 1$ with $\Gamma_1' = 1/\Gamma_1$ they can be expressed [9] in terms of the tangential field components as

$$E_x = \Gamma_1 Z H_z \quad , \qquad E_z = -\Gamma_1 Z H_x \tag{6}$$

implying

$$\hat{n} \times (\hat{n} \times \bar{E}) = -\Gamma_1 Z \hat{n} \times \bar{H}$$

where $\hat{n}$ is the unit vector outward normal to the surface. This provides the needed extension to a non-planar surface and is the form in which an impedance boundary condition is usually stated. In a similar manner, any pair of generalized boundary conditions can be expressed in terms of the tangential field components provided Γ_m

and Γ_m' are appropriately related, and to illustrate the procedure, we consider the second order case.

The boundary condition for E_y is

$$\left\{\frac{\partial^2}{\partial y^2} + ik(\Gamma_1 + \Gamma_2)\frac{\partial}{\partial y} - k^2\Gamma_1\Gamma_2\right\} E_y = 0 \quad ,$$

and using Maxwell's equations and the fact that $\nabla \cdot \bar{E} = 0$, this can be written as

$$\frac{\partial}{\partial x}\left\{E_x - \frac{\Gamma_1\Gamma_2 + 1}{\Gamma_1 + \Gamma_2} ZH_z + \frac{1}{ik(\Gamma_1 + \Gamma_2)}\frac{\partial E_y}{\partial x} + \frac{\partial f}{\partial z}\right\}$$

$$= -\frac{\partial}{\partial z}\left\{E_z + \frac{\Gamma_1\Gamma_2 + 1}{\Gamma_1 + \Gamma_2} ZH_x + \frac{1}{ik(\Gamma_1 + \Gamma_2)}\frac{\partial E_y}{\partial z} - \frac{\partial f}{\partial x}\right\} \qquad (7)$$

for any function $f = f(x,z)$. Similarly, from the boundary condition for H_y,

$$\frac{\partial}{\partial x}\left\{H_x + \frac{\Gamma_1'\Gamma_2' + 1}{\Gamma_1' + \Gamma_2'} YE_z + \frac{1}{ik(\Gamma_1' + \Gamma_2')}\frac{\partial H_y}{\partial x} + \frac{\partial g}{\partial z}\right\}$$

$$= -\frac{\partial}{\partial z}\left\{H_z - \frac{\Gamma_1'\Gamma_2' + 1}{\Gamma_1' + \Gamma_2'} YE_x + \frac{1}{ik(\Gamma_1' + \Gamma_2')}\frac{\partial H_y}{\partial z} - \frac{\partial g}{\partial x}\right\} \quad ,$$

and therefore

$$\frac{\partial}{\partial z}\left\{E_x - \frac{\Gamma_1' + \Gamma_2'}{\Gamma_1'\Gamma_2' + 1} ZH_z + \frac{\Gamma_1' + \Gamma_2'}{\Gamma_1'\Gamma_2' + 1} Z\frac{\partial g}{\partial x} - \frac{1}{ik(\Gamma_1'\Gamma_2' + 1)} Z\frac{\partial H_y}{\partial z}\right\}$$

$$= \frac{\partial}{\partial x}\left\{ E_z + \frac{\Gamma_1' + \Gamma_2'}{\Gamma_1'\Gamma_2' + 1} ZH_x + \frac{\Gamma_1' + \Gamma_2'}{\Gamma_1'\Gamma_2' + 1} Z\frac{\partial g}{\partial z} + \frac{1}{ik(\Gamma_1'\Gamma_2' + 1)} Z\frac{\partial H_y}{\partial x} \right\} \qquad (8)$$

for any function g = g (x,z). Choose now

$$f = -\frac{1}{ik(\Gamma_1'\Gamma_2' + 1)} ZH_y$$

and

$$g = \frac{\Gamma_1'\Gamma_2' + 1}{\Gamma_1' + \Gamma_2'} \quad \frac{1}{ik(\Gamma_1 + \Gamma_2)} YE_y \quad .$$

Then, if

$$\frac{\Gamma_1' + \Gamma_2'}{\Gamma_1'\Gamma_2' + 1} = \frac{\Gamma_1\Gamma_2 + 1}{\Gamma_1 + \Gamma_2} \quad , \qquad (9)$$

(7) and (8) imply

$$\left(\frac{\partial^2}{\partial x^2} + \frac{\partial^2}{\partial z^2}\right)\left\{ E_x - \frac{\Gamma_1\Gamma_2 + 1}{\Gamma_1 + \Gamma_2} ZH_z + \frac{1}{ik(\Gamma_1 + \Gamma_2)} \frac{\partial E_y}{\partial x} - \frac{1}{ik(\Gamma_1'\Gamma_2' + 1)} Z\frac{\partial H_y}{\partial z} \right\} = 0$$

$$\left(\frac{\partial^2}{\partial x^2} + \frac{\partial^2}{\partial z^2}\right)\left\{ E_z + \frac{\Gamma_1\Gamma_2 + 1}{\Gamma_1 + \Gamma_2} ZH_x + \frac{1}{ik(\Gamma_1 + \Gamma_2)} \frac{\partial E_y}{\partial z} + \frac{1}{ik(\Gamma_1'\Gamma_2' + 1)} Z\frac{\partial H_y}{\partial x} \right\} = 0 \quad ,$$

and as shown in [2], the only allowed solutions of these equations are zero.

Hence

$$E_x = \frac{\Gamma_1\Gamma_2 + 1}{\Gamma_1 + \Gamma_2} ZH_z - \frac{1}{ik(\Gamma_1 + \Gamma_2)} \frac{\partial E_y}{\partial x} + \frac{1}{ik(\Gamma_1'\Gamma_2' + 1)} Z \frac{\partial H_y}{\partial z} \tag{10}$$

$$E_z = - \frac{\Gamma_1\Gamma_2 + 1}{\Gamma_1 + \Gamma_2} ZH_x - \frac{1}{ik(\Gamma_1 + \Gamma_2)} \frac{\partial E_y}{\partial z} - \frac{1}{ik(\Gamma_1'\Gamma_2' + 1)} Z \frac{\partial H_y}{\partial x} \tag{11}$$

on $y = 0$. We note that the relation (9) connecting the Γ_m and Γ_m' is equivalent to

$$\frac{a_1'}{a_2' + a_0'} = \frac{a_2 + a_0}{a_1} , \tag{12}$$

and is a consequence of duality.

The vector form of (10) and (11) is

$$\hat{n} \times \left(\hat{n} \times \left\{ \bar{E} + \frac{1}{ika_1} \nabla [\hat{n} \cdot \bar{E}] \right\} \right) = - \frac{a_2 + a_0}{a_1} Z \hat{n} \times \left\{ \bar{H} + \frac{1}{ika_1'} \nabla [\hat{n} \cdot \bar{H}] \right\} \tag{13}$$

and this provides the extension of the second order conditions to a non-planar surface since (13) is now geometry independent. Similarly, in the third order case we obtain

$$\hat{n} \times \left(\hat{n} \times \left\{ \bar{E} + \frac{1}{ik(a_3 + a_1)} \nabla \left[a_2 \hat{n} \cdot \bar{E} - \frac{1}{ik} \nabla_s \cdot \bar{E} \right] \right\} \right)$$

$$= - \frac{a_2 + a_0}{a_3 + a_1} Z \hat{n} \times \left\{ \bar{H} + \frac{1}{ik(a_3' + a_1')} \nabla \left[a_2' \hat{n} \cdot \bar{H} - \frac{1}{ik} \nabla_s \cdot \bar{H} \right] \right\} \tag{14}$$

provided

$$\frac{a_3' + a_1'}{a_2' + a_0'} = \frac{a_2 + a_0}{a_3 + a_1} \tag{15}$$

or, equivalently,

$$\frac{\Gamma_1' + \Gamma_2' + \Gamma_3' + \Gamma_1'\Gamma_2'\Gamma_3'}{\Gamma_1'\Gamma_2' + \Gamma_2'\Gamma_3' + \Gamma_3'\Gamma_1' + 1} = \frac{\Gamma_1\Gamma_2 + \Gamma_2\Gamma_3 + \Gamma_3\Gamma_1 + 1}{\Gamma_1 + \Gamma_2 + \Gamma_3 + \Gamma_1\Gamma_2\Gamma_3} \tag{16}$$

where ∇_s is the surface divergence. The extension of (13) and (14) to still higher order boundary conditions is obvious. It is evident from the above that one effect of going to higher order boundary conditions is to make them less local through the inclusion of tangential derivatives of the fields.

4. Metal-Backed Layer

A geometry of practical interest is a uniform dielectric layer of thickness τ backed by a metal (see Figure 1), and we now seek a simulation using generalized boundary conditions of the form (1) or (2). In doing so, particular attention is given to layers of reasonable thickness since, as discussed below, approximate boundary conditions are already available for very thin coatings. For this geometry the exact reflection coefficients are known, and we can therefore derive the conditions using procedure (i). These can be referred either to the surface y = 0+ of the dielectric layer or, by using the expansion (5), to the surface y = -τ+ of the metal backing (note that (5) is applicable here only after letting $\tau \rightarrow -\tau$).

For an H-polarized plane wave having $E_y \neq 0$ the reflection coefficient is

$$R(\phi) = - \frac{\sqrt{N^2 - \cos^2\phi}\ \tan\left(k\tau\sqrt{N^2 - \cos^2\phi}\right) - i\varepsilon \sin\phi}{\sqrt{N^2 - \cos^2\phi}\ \tan\left(k\tau\sqrt{N^2 - \cos^2\phi}\right) + i\varepsilon \sin\phi} \tag{17}$$

where $N = \sqrt{\varepsilon\mu}$ is the complex refractive index, ε is the relative permittivity and μ is the relative permeability of the layer. The corresponding reflection coefficient for E-polarization is

$$R'(\phi) = - \frac{\sqrt{N^2 - \cos^2\phi}\ \cot\left(k\tau\sqrt{N^2 - \cos^2\phi}\right) + i\mu \sin\phi}{\sqrt{N^2 - \cos^2\phi}\ \cot\left(k\tau\sqrt{N^2 - \cos^2\phi}\right) - i\mu \sin\phi} \tag{18}$$

where $R(\phi)$ and $R'(\phi)$ are both referred to $y = 0+$. Expansion of the tangent and cotangent in powers of $\sin\phi$ leads immediately to the identification of the constants a_m and a'_m, but before doing this, it is of interest to examine two boundary conditions already available in the literature.

The most commonly-used boundary condition for simulating a metal-backed layer is the standard impedance condition [1]. This is a first order one which can be derived from (15) and (16) by writing $\sqrt{N^2 - \cos^2\phi} \approx N$, giving

$$\Gamma_1 = \frac{1}{\Gamma'_1} = - i \frac{N}{\varepsilon} \tan(Nk\tau) \tag{19}$$

with all other $\Gamma_m = 0$. For $k\tau < 0.52$ the conditions can be transferred to the surface $y = -\tau+$ with a maximum phase error of 10 degrees by employing the first two terms in (5). The resulting boundary conditions are then second order ones in which Γ_1 and Γ_1' remain the same and Γ_2 and $\Gamma_2' = (ik\tau)^{-1}$. These have been used [4] to simulate a metal-backed dielectric half-plane and since they are valid only if $|N| >> 1$, they will be referred to as high contrast conditions. Low contrast conditions can be derived by introducing the approximations $\tan x \approx x$ and $\cot x \approx 1/x$ in (17) and (18), giving

$$R(\phi) \approx - \frac{k\tau \sin^2\phi - i\varepsilon \sin\phi + k\tau (N^2 - 1)}{k\tau \sin^2\phi + i\varepsilon \sin\phi + k\tau (N^2 - 1)}$$

and

$$R'(\phi) \approx \frac{ik\tau \mu \sin\phi + 1}{ik\tau \mu \sin\phi - 1} ,$$

from which the constants a_m and a_m' are easily found. The corresponding boundary conditions can be transferred to the surface $y = -\tau+$ using the first two terms in the expansion (5), and when only the terms of leading order in $k\tau$ are retained, the constants are

$$\begin{aligned} a_0 &= k\tau (N^2 - 1) & a_0' &= 1 \\ a_1 &= i\varepsilon & a_1' &= -ik\tau (\mu - 1) \\ a_2 &= -k\tau (\varepsilon - 1) & a_2' &= 0 . \end{aligned} \qquad (20)$$

These satisfy (11) and the resulting boundary conditions are identical to those derived by Weinstein [3] by expanding the fields in the dielectric as Taylor series in y.

The high and low contrast boundary conditions provide an accurate simulation of the coating over the entire angular range only for limited ranges of |N| and $k\tau$. However, by going to a higher order condition, it is possible to produce a simulation that is valid for all |N| and a wider range of $k\tau$. To this end we write

$$\sqrt{N^2 - \cos^2\phi} \approx N - \frac{1}{2N} + \frac{\sin^2\phi}{2N} \quad .$$

By also employing the approximation

$$\tan\left(\frac{k\tau}{2N}\sin^2\phi\right) \approx \frac{k\tau}{2N}\sin^2\phi \quad ,$$

$R(\phi)$ can be expressed as

$$R(\phi) = -\frac{\sum_{m=0}^{4}(-1)^m a_m \sin^m\phi}{\sum_{m=0}^{4} a_m \sin^m\phi} \qquad (21)$$

where

$$a_0 = (N - \frac{1}{2N})\left[\tan(k\tau N) - \tan(\frac{k\tau}{2N})\right]$$

$$a_1 = i\varepsilon\left[1 + \tan(k\tau N)\tan(\frac{k\tau}{2N})\right]$$

$$a_2 = \frac{1}{2N}\left\{\tan(k\tau N) - \tan\left(\frac{k\tau}{2N}\right) + k\tau\left(N - \frac{1}{2N}\right)\left[1 + \tan(k\tau N)\tan\left(\frac{k\tau}{2N}\right)\right]\right\} \qquad (22)$$

$$a_3 = -\frac{ik\tau\varepsilon}{2N}\left[\tan(k\tau N) - \tan\left(\frac{k\tau}{2N}\right)\right]$$

$$a_4 = \frac{k\tau}{4N^2}\left[1 + \tan(k\tau N)\tan\left(\frac{k\tau}{2N}\right)\right] .$$

Similarly, for E-polarization,

$$a_0' = (2N^2 - 1)\left[1 + \cot(k\tau N)\cot\left(\frac{k\tau}{2N}\right)\right]$$

$$a_1' = i\,2N\mu\left[\cot(k\tau N) - \cot\left(\frac{k\tau}{2N}\right)\right]$$

$$a_2' = 1 + \cot(k\tau N)\cot\left(\frac{k\tau}{2N}\right) + k\tau\left(N - \frac{1}{2N}\right)\left[\cot(k\tau N) - \cot\left(\frac{k\tau}{2N}\right)\right] \qquad (23)$$

$$a_3' = -i\,k\tau\mu\left[1 + \cot(k\tau N)\cot\left(\frac{k\tau}{2N}\right)\right]$$

$$a_4' = \frac{k\tau}{2N}\left[\cot(k\tau N) - \cot\left(\frac{k\tau}{2N}\right)\right] .$$

The boundary conditions implied by (22) and (23) are referred to the surface $y = 0+$ and are fourth order ones which satisfy duality. As expected, their accuracy improves with increasing $|N|/(k\tau)$ and in Figure 2 it is shown that they predict the correct reflection coefficient for $\varepsilon = 4$, $\mu = 1$ and $\tau = 0.1\lambda$, i.e., $Nk\tau = 1.26$. When we set $a_3 = a_4 = 0$ and $a_3' = a_4' = 0$ the resulting boundary conditions are second order ones. As evident from Figure 2, their accuracy is substantially less, and the standard impedance (first order) conditions are valid only for incidence close to grazing or normal.

The accuracy of the fourth order boundary conditions is quite remarkable even for fairly thick coatings. Since the conditions correctly predict the dominant surface wave modes (see comment below), their accuracy is greatest near grazing incidence, but even at other angles the phase error is less than 2 degrees with coatings up to $\lambda/4$ thick for either polarization and material composition provided $|N| > 2$. This is illustrated in Figures 3 and 4 where, for $\varepsilon = 2$ and 7 with μ real, the maximum layer thickness for a 2-degree phase error is shown as a function of $|N|$ for $\phi = 90$ and 45 degrees, respectively. It should be noted, in contrast to the standard impedance boundary condition, the accuracy of the conditions specified by the constants (22) - (23) is least at normal incidence and increases with the refractive index and loss in the material coating.

If a 10 degree error in phase and/or 10% in magnitude is acceptable, a truncated form of the fourth order conditions implied by (22) - (23) become useful. Figures 5 to 10 show the maximum thickness for which the second order (truncated from the fourth) condition is capable of predicting the coating's plane wave reflection coefficient within 10 degrees of its actual phase and/or 10% of its actual magnitude. As seen, in comparison with the standard impedance boundary condition, the second order condition provides substantially better accuracy for incidence angles away from normal. Notably, the simulation improves monotonically as one approaches grazing. We may conclude from Figures 5 to 7 that for H-polarization, the second order condition is capable of simulating coatings having thickness up to 1/5 of a wavelength for incidence angles greater than 35° from normal (55° from grazing). This is regardless of the dielectric's properties since the simulation improves substantially as

N and/or the loss in the coating increases. In contrast, the 1st order (standard impedance) condition provides a superior simulation with respect to the second order condition for the rest of the angular region (i.e. within 35° from normal). Turning to Figures 8 to 10 one again arrives at similar conclusions for E-polarization. However, it should be noted that for small N the deterioration of the simulation provided by the second order condition as normal incidence is approached, is now more rapid.

Figures 11 to 13 show the maximum thickness for which the third order condition is capable of predicting the coating's plane wave reflection coefficient within 10 degrees and/or 10% of its magnitude. It is observed that this condition provides an acceptable simulation for coating thickness of at least 0.4λ regardless of material properties, angle of incidence and polarization.

For the standard impedance boundary condition, results analogous to those in Figure 4 are shown in Figure 14. Even with the allowed phase error increased to 10 degrees, the maximum layer thickness is substantially less except at normal incidence, particularly if $|N|$ is small. In addition, the accuracy of this boundary condition decreases as grazing incidence is approached.

Higher order boundary conditions for a metal-backed layer can also be derived using procedure (ii) of Section 2, which requires a knowledge of the complex poles of the reflection coefficients (17) and (18). The subset lying in the proper half of the complex plane are the usual surface wave poles, and the implied expansions of the reflection coefficients are

$$R(\phi) = -\sum_{m=0}^{M} \frac{\sin\theta_m - \sin\phi}{\sin\theta_m + \sin\phi}$$

$$R'(\phi) = -\sum_{m=0}^{M'} \frac{\sin\theta'_m - \sin\phi}{\sin\theta'_m + \sin\phi} \qquad (24)$$

where $f_m = -ik \sin\theta_m$ and $f'_m = -ik \sin\theta'_m$ are the propagation constants for the H-polarized (TM) and E-polarized (TE) surface waves, respectively, provided Re. $(f_m, f'_m) > 0$.

It has been observed that the accuracy of the approximate boundary conditions deteriorates significantly as ϕ decreases unless the correct dominant surface wave fields are predicted, and the boundary conditions implied by (22) and (23) must therefore correspond to the correct surface wave poles. The number of poles (or zeros) of the reflection coefficients (17) and (18) depends on the value of Re. $(k\tau N)$. In the TM case with $k\tau N$ small, only one pole exists corresponding to the lowest order surface wave mode. As $k\tau N$ increases, two additional poles appear, one of which is associated with a surface wave mode when $u > \pi$ where $u^2 = (k\tau)^2 (N^2 - 1) - \sin^2\phi$. In the TE case, no poles exist for small $k\tau N$, but as $k\tau N$ increases, two poles appear simultaneously, and one of these is associated with the lowest order TE surface wave mode when $u > \pi/2$. An examination of the accuracy of (24) showed that they provide a good simulation of the reflection coefficients for those values of $k\tau N$ such that the corresponding poles (with $\sin\theta_m$, $\sin\theta'_m$ not much greater

than unity) have just appeared; however, the accuracy decreases substantially as $k\tau N$ increases beyond the mid point between the last included pole and the next one to appear.

5. Multilayer Metal-Backed Coating

Of more practical interest is the simulation of multilayer coatings and in this section we consider the derivation of higher order boundary conditions applicable to a three layer coating with arbitrary constitutive parameters. The geometry of the coating is illustrated in Figure 15. For E-polarization ($H_y \neq 0$) the plane wave reflection coefficient referenced to $y = 0^+$ can be written as

$$R'(\phi) = \frac{F'_N(\phi)}{F'_D(\phi)} \tag{25}$$

where

$$\begin{aligned}
\frac{F'_N}{D}(\phi) = {} & -i\mu_1\mu_2\mu_3 k_{y0}k_{y1}k_{y2} \sin(k_{y3}\tau_3)\cos(k_{y2}\tau_2)\cos(k_{y1}\tau_1) \\
& + i\mu_1^2\mu_3 k_{y0}k_{y2}^2 \sin(k_{y3}\tau_3)\sin(k_{y2}\tau_2)\sin(k_{y1}\tau_1) \\
& - i\mu_1\mu_2^2 k_{y0}k_{y1}k_{y3} \cos(k_{y3}\tau_3)\sin(k_{y2}\tau_2)\cos(k_{y1}\tau_1) \\
& - i\mu_1^2\mu_2 k_{y0}k_{y2}k_{y3} \cos(k_{y3}\tau_3)\cos(k_{y2}\tau_2)\sin(k_{y1}\tau_1) \\
& \pm \mu_2\mu_3 k_{y1}^2 k_{y2} \sin(k_{y3}\tau_3)\cos(k_{y2}\tau_2)\sin(k_{y1}\tau_1) \\
& \pm \mu_1\mu_3 k_{y1}k_{y2}^2 \sin(k_{y3}\tau_3)\sin(k_{y2}\tau_2)\cos(k_{y1}\tau_1) \\
& \pm \mu_2^2 k_{y1}^2 k_{y3} \cos(k_{y3}\tau_3)\sin(k_{y2}\tau_2)\sin(k_{y1}\tau_1)
\end{aligned}$$

$$\mp\mu_1\mu_2 k_{y1} k_{y2} k_{y3} \cos(k_{y3}\tau_3) \cos(k_{y2}\tau_2) \cos(k_{y1}\tau_1) \qquad (26)$$

In the above (μ_n, ε_n) are the relative constitutive parameters of the nth layer with n = 1 corresponding to the top layer, t_n denotes the thickness of the nth layer, and

$$k_{yn} = k\sqrt{N_n^2 - \cos^2\phi} \qquad (27)$$

with $N_n = \sqrt{\mu_n \varepsilon_n}$ and $k_{y0} = k \sin\phi$. As before, ϕ is measured from the surface of the coating.

Similarly, for H-polarization ($E_y \neq 0$) the corresponding reflection coefficient referenced to $y = 0^+$ is given as

$$R(\phi) = \frac{F_N(\phi)}{F_D(\phi)} \qquad (28)$$

where now

$$\begin{aligned}
\frac{F_N}{D}(\phi) = {} & \varepsilon_1\varepsilon_2\varepsilon_3 k_{y0} k_{y1} k_{y2} \cos(k_{y3}\tau_3) \cos(k_{y2}\tau_2) \cos(k_{y1}\tau_1) \\
& -\varepsilon_1^2\varepsilon_3 k_{y0} k_{y2}^2 \cos(k_{y3}\tau_3) \sin(k_{y2}\tau_2) \sin(k_{y1}\tau_1) \\
& -\varepsilon_1\varepsilon_2^2 k_{y0} k_{y1} k_{y3} \sin(k_{y3}\tau_3) \sin(k_{y2}\tau_2) \cos(k_{y1}\tau_1) \\
& -\varepsilon_1^2\varepsilon_2 k_{y0} k_{y2} k_{y3} \sin(k_{y3}\tau_3) \cos(k_{y2}\tau_2) \sin(k_{y1}\tau_1) \\
& \pm i\varepsilon_2\varepsilon_3 k_{y1}^2 k_{y2} \cos(k_{y3}\tau_3) \cos(k_{y2}\tau_2) \sin(k_{y1}\tau_1) \\
& \pm i\varepsilon_1\varepsilon_3 k_{y1} k_{y2}^2 \cos(k_{y3}\tau_3) \sin(k_{y2}\tau_2) \cos(k_{y1}\tau_1) \\
& \mp i\varepsilon_2^2 k_{y1}^2 k_{y3} \sin(k_{y3}\tau_3) \sin(k_{y2}\tau_2) \sin(k_{y1}\tau_1) \\
& \pm i\varepsilon_1\varepsilon_2 k_{y1} k_{y2} k_{y3} \sin(k_{y3}\tau_3) \cos(k_{y2}\tau_2) \cos(k_{y1}\tau_1) \qquad (29)
\end{aligned}$$

To find the constants a_m and a_m' appearing in (2) and (3) we must expand the terms $\sin(k_{yn}\tau_n)$ and $\cos(k_{yn}\tau_n)$ in powers of $\sin\phi$. The simplest case is to assume that $k_{yn}t_n$ is sufficiently small so that we may set

$$\sin(k_{yn}\tau_n) \approx k_{yn}\tau_n \tag{30}$$

and

$$\cos(k_{yn}\tau_n) \approx 1 \tag{31}$$

By retaining only terms of $O(\tau_n)$ we obtain

$$\begin{aligned} a_0 &= \frac{(N_1^2 - 1)\,k\tau_1}{\varepsilon_1} + \frac{(N_2^2 - 1)\,k\tau_2}{\varepsilon_2} + \frac{(N_3^2 - 1)\,k\tau_3}{\varepsilon_3} \\ a_1 &= +i \\ a_3 &= k\left(\frac{\tau_1}{\varepsilon_1} + \frac{\tau_2}{\varepsilon_2} + \frac{\tau_3}{\varepsilon_3}\right) \end{aligned} \tag{32}$$

and

$$\begin{aligned} a_0' &= 1 \\ a_1' &= -ik\,(\mu_1\tau_1 + \mu_2\tau_2 + \mu_3\tau_3) \\ a_2' &= 0 \quad . \end{aligned} \tag{33}$$

The last set of constants imply a first order condition, but by retaining all terms of the expansion we find that

$$\begin{aligned} a_0' &= \mu_1\mu_2 - \alpha_1\,(N_1^2 - 1) - \alpha_2\,(N_2^2 - 1) \\ a_1' &= -ik\,\mu_1\mu_2\,(\mu_1\tau_1 + \mu_2\tau_2 + \mu_3\tau_3) \\ a_2' &= -\,(\alpha_1 + \alpha_2) \end{aligned} \tag{34}$$

in which

$$\alpha_1 = k^2 \mu_1\mu_3 \tau_2 \ [\mu_1 k \tau_1\tau_3 + \tau_3]$$

and (35)

$$\alpha_2 = k^2 \mu_2 \tau_1 [\mu_2 \tau_2 + \mu_3 \tau_3] \ .$$

It is obviously expected that (34) will allow the simulation of thicker layers than (33).

By their derivation, the boundary conditions implied by the constants in (32), (33) or (34) are applicable to very thin coatings ($k \sum t_n \leq 0.6$) with moderate values of N_n. However, as noted earlier for the single layer coating, higher order conditions are required to allow simulations which remain valid for a wider range of N_n and kt_n. To derive a higher order condition for the three layer coating, we may parallel the approach employed for the single layer coating and set

$$k_n = k\sqrt{N_n^2 - \cos^2\phi} \approx k\left(N_n - \frac{1}{2N_n} + \frac{\sin^2\phi}{2N_n}\right) \tag{36}$$

This, however, will lead to 12th order condition that is obviously impractical to employ analytically or numerically. Instead, a more reasonable approach is to assume that the three layers comprising the coating have varying refractive indices. In practice the top layer is low contrast dielectric, whereas the bottom layer may be a high contrast dielectric. With this assumption we may then set

$$\sin(k_y, \tau_1) \approx k_{y1} \tau_1$$

$$\cos(k_{y1} \tau_1) \approx 1$$

$$k_{y2} = k\sqrt{N_2^2 - \cos^2\phi} \approx k\left(N_2 - \frac{1}{2N_2} + \frac{\sin^2\phi}{2N_2}\right)$$

$$\sin\left(\frac{k\tau_2}{2N_2}\sin^2\phi\right) \approx \frac{k\tau_2}{2N_2}\sin^2\phi$$

$$\cos\left(\frac{k\tau_2}{2N_2}\sin^2\phi\right) \approx 1$$

and

$$k_{y3} = k\sqrt{N_3^2 - \cos^2\phi} \approx k\ N_3 \tag{37}$$

Employing the above approximations in (26) - (29) after much tedious algebra we find that R (ϕ) and R' (ϕ) may be written as

$$R(\phi) = -\frac{\sum_{m=0}^{6}(-1)^m a_m \sin^m\phi}{\sum_{m=0}^{6} a_m \sin^m\phi} \tag{38}$$

and

$$R'(\phi) = -\frac{\sum_{m=0}^{6}(-1)^m a'_m \sin^m\phi}{\sum_{m=0}^{6} a'_m \sin^m\phi} \tag{39}$$

implying a sixth order condition. For H-polarization, the constants are given by

$$a_o = i\,\varepsilon_2\,\varepsilon_3\,(N_1^2 - 1)\left(N_2 - \frac{1}{2N_2}\right)\tau_1$$

$$i\,\varepsilon_1\,\varepsilon_3\,(N_2^2 - 1)\tan\left[\left(N_2 - \frac{1}{2N_2}\right)k\,\tau_2\right]$$

$$-i\,\varepsilon_2^2\,(N_1^2-1)\,N_3\,\tau_1\tan\left[\left(N_2-\frac{1}{2N_2}\right)k\,\tau_2\right]\tan\left(N_3\,k\,\tau_3\right)$$

$$i\,\varepsilon_1\,\varepsilon_2\left(N_2-\frac{1}{2N_2}\right)N_3\tan\left(N_3\,k\,\tau_3\right) \qquad (40)$$

$$a_1 = -\,\varepsilon_1\,\varepsilon_2\,\varepsilon_3\left(N_2-\frac{1}{2N_2}\right)$$

$$+\varepsilon_1^2\,\varepsilon_3\,(N_2^2-1)\,\tau_1\tan\left[\left(N_2-\frac{1}{2N_2}\right)k\,\tau_2\right]$$

$$+\varepsilon_1\,\varepsilon_2^2\,N_3\tan\left[\left(N_2-\frac{1}{2N_2}\right)k\,\tau_2\right]\tan\left(N_3\,k\,\tau_3\right)$$

$$+\varepsilon_1^2\,\varepsilon_2\left(N_2-\frac{1}{2N_2}\right)N_3\,\tau_1\tan\left(N_3\,k\,\tau_3\right) \qquad (41)$$

$$a_2 = -i\,\varepsilon_2\,\varepsilon_3\,(N_1^2-1)\left(N_2-\frac{1}{2N_2}\right)\tau_1\frac{k\,\tau_2}{2N_2}\tan\left[\left(N_2-\frac{1}{2N_2}\right)k\,\tau_2\right]$$

$$+i\,\varepsilon_2\,\varepsilon_3\left(N_2-\frac{1}{2N_2}\right)\tau_1 + i\,\varepsilon_2\,\varepsilon_3\,(N_1^2-1)\frac{1}{2N_2}\tau_1$$

$$+i\,\varepsilon_1\,\varepsilon_3\,(N_2^2-1)\frac{k\,\tau_2}{2N_2} + i\,\varepsilon_1\varepsilon_3\tan\left[\left(N_2-\frac{1}{2N_2}\right)k\,\tau_2\right]$$

$$-i\,\varepsilon_2^2\,(N_1^2-1)\,N_3\,\tau_1\frac{k\,\tau_2}{2N_2}\tan\left(N_3\,k\,\tau_3\right)$$

$$-i\,\varepsilon_2^2\,N_3\,\tau_1\tan\left[\left(N_2-\frac{1}{2N_2}\right)k\,\tau_2\right]\tan\left(N_3\,k\,\tau_3\right)$$

$$-i\,\varepsilon_1\,\varepsilon_2\left(N_2-\frac{1}{2N_2}\right)N_3\frac{k\,\tau_2}{2N_2}\tan\left[\left(N_2-\frac{1}{2N_2}\right)k\,\tau_2\right]\tan\left(N_3\,k\,\tau_3\right)$$

$$+i\,\varepsilon_1\,\varepsilon_2\frac{1}{2N_2}N_3\tan\left(N_3\,k\,\tau_3\right) \qquad (42)$$

$$a_3 = -\varepsilon_1 \varepsilon_2 \varepsilon_3 \frac{1}{2N_2} + \varepsilon_1 \varepsilon_2 \varepsilon_3 \left(N_2 - \frac{1}{2N_2}\right) \frac{k\tau_2}{2N_2} \tan\left[\left(N_2 - \frac{1}{2N_2}\right) k\tau_2\right]$$

$$+ \varepsilon_1^2 \varepsilon_3 \tau_1 \tan\left[\left(N_2 - \frac{1}{2N_2}\right) k\tau_2\right] + \varepsilon_1^2 \varepsilon_3 (N_2^2 - 1) \frac{k\tau_2}{2N_2}$$

$$+ \varepsilon_1 \varepsilon_2^2 N_3 \frac{k\tau_2}{2N_2} \tan(N_3 k\tau_3)$$

$$- \varepsilon_1^2 \varepsilon_2 \left(N_2 - \frac{1}{2N_2}\right) N_3 \tau_1 \frac{k\tau_2}{2N_2} \tan\left[\left(N_2 - \frac{1}{2N_2}\right) k\tau_2\right] \tan(N_3 k\tau_3)$$

$$+ \varepsilon_1^2 \varepsilon_2 \frac{1}{2N_2} N_3 \tau_1 \tan(N_3 k\tau_3) \qquad (43)$$

$$a_4 = -i \varepsilon_2 \varepsilon_3 (N_1^2 - 1) \frac{1}{2N_2} \tau_1 \frac{k\tau_2}{2N_2} \tan\left[\left(N_2 - \frac{1}{2N_2}\right) k\tau_2\right]$$

$$-i \varepsilon_2 \varepsilon_3 \left(N_2 - \frac{1}{2N_2}\right) \tau_1 \frac{k\tau_2}{2N_2} \tan\left[\left(N_2 - \frac{1}{2N_2}\right) k\tau_2\right]$$

$$+i \varepsilon_2 \varepsilon_3 \frac{1}{2N_2} \tau_1 + i \varepsilon_1 \varepsilon_3 \frac{k\tau_2}{2N_2}$$

$$-i \varepsilon_2^2 N_3 \tau_1 \frac{k\tau_2}{2N_2} \tan(N_3 k\tau_3)$$

$$-i \varepsilon_1 \varepsilon_2 \frac{1}{2N_2} N_3 \frac{k\tau_2}{2N_2} \tan\left[\left(N_2 - \frac{1}{2N_2}\right) k\tau_2\right] \tan(N_3 k\tau_3) \qquad (44)$$

$$a_5 = \varepsilon_1 \varepsilon_2 \varepsilon_3 \frac{1}{2N_2} \frac{k\tau_2}{2N_2} \tan\left[\left(N_2 - \frac{1}{2N_2}\right) k\tau_2\right]$$

$$+ \varepsilon_1^2 \varepsilon_3 \tau_1 \frac{k\tau_2}{2N_2}$$

$$- \varepsilon_1^2 \varepsilon_2 \frac{1}{2N_2} N_3 \tau_1 \frac{k\tau_2}{2N_2} \tan\left[\left(N_2 - \frac{1}{2N_2}\right) k\tau_2\right] \tan\left(N_3 k \tau_3\right) \tag{45}$$

$$a_6 = -i \varepsilon_2 \varepsilon_3 \frac{1}{2N_2} \tau_1 \frac{k\tau_2}{2N_2} \tan\left[\left(N_2 - \frac{1}{2N_2}\right) k\tau_2\right] \tag{46}$$

Similarly, for E-polarization, we find

$$\begin{aligned} a_0' = {} & \mu_2 \mu_3 (N_1^2 - 1) \left(N_2 - \frac{1}{2N_2}\right) \tau_1 \tan\left(N_3 k \tau_3\right) \\ & + \mu_1 \mu_3 (N_2^2 - 1) \tan\left[\left(N_2 - \frac{1}{2N_2}\right) k \tau_2\right] \tan\left(N_3 k \tau_3\right) \\ & + \mu_2^2 (N_1^2 - 1) N_3 \tau_1 \tan\left[\left(N_2 - \frac{1}{2N_2}\right) k \tau_2\right] \\ & - \mu_1 \mu_2 \left(N_2 - \frac{1}{2N_2}\right) N_3 \end{aligned} \tag{47}$$

$$\begin{aligned} a_1' = {} & + i \mu_1 \mu_2 \mu_3 \left(N_2 - \frac{1}{2N_2}\right) \tan\left(N_3 k \tau_3\right) \\ & - i \mu_1^2 \mu_3 (N_2^2 - 1) \tau_1 \tan\left[\left(N_2 - \frac{1}{2N_2}\right) k_o \tau_2\right] \tan\left(N_3 k_o \tau_3\right) \\ & + i \mu_1 \mu_2^2 N_3 \tan\left[\left(N_2 - \frac{1}{2N_2}\right) k_o \tau_2\right] \\ & + i \mu_1^2 \mu_2 \left(N_2 - \frac{1}{2N_2}\right) N_3 \tau_1 \end{aligned} \tag{48}$$

$$\begin{aligned} a_2' = {} & \mu_2 \mu_3 (N_1^2 - 1) \frac{1}{2N_2} \tau_1 \tan\left(N_3 k \tau_3\right) \\ & + \mu_2 \mu_3 \left(N_2 - \frac{1}{2N_2}\right) \tau_1 \tan\left(N_3 k_o \tau_3\right) \end{aligned}$$

$$- \mu_2 \mu_3 (N_1^2 - 1) \left(N_2 - \frac{1}{2N_2}\right) \tau_1 \frac{k\tau_2}{2N_2} \tan\left[\left(N_2 - \frac{1}{2N_2}\right) k\tau_2\right] \tan(N_3 k\tau_3)$$

$$+ \mu_1 \mu_3 \tan\left[\left(N_2 - \frac{1}{2N_2}\right) k\tau_2\right] \tan(N_3 k\tau_3)$$

$$+ \mu_1 \mu_3 (N_2^2 - 1) \frac{k\tau_2}{2N_2} \tan(N_3 k\tau_3)$$

$$+ \mu_2^2 N_3 \tau_1 \tan\left[\left(N_2 - \frac{1}{2N_2}\right) k\tau_2\right] + \mu_2^2 (N_2^2 - 1) N_3 \tau_1 \frac{k\tau_2}{2N_2}$$

$$- \mu_1 \mu_2 \frac{1}{2N_2} N_3 + \mu_1 \mu_2 \left(N_2 - \frac{1}{2N_2}\right) N_3 \frac{k\tau_2}{2N_2} \tan\left[\left(N_2 - \frac{1}{2N_2}\right) k\tau_2\right] \qquad (49)$$

$$a_3 = - i \mu_1 \mu_2 \mu_3 \left(N_2 - \frac{1}{2N_2}\right) \frac{k\tau_2}{2N_2} \tan\left[\left(N_2 - \frac{1}{2N_2}\right) K\tau_2\right] \tan(N_3 k\tau_3)$$

$$+i \mu_1 \mu_2 \mu_3 \frac{1}{2N_2} \tan(N_3 k\tau_3)$$

$$-i \mu_1^2 \mu_3 (N_2^2 - 1) \tau_1 \frac{k\tau_2}{2N_2} \tan(N_3 k\tau_3)$$

$$-i \mu_1^2 \mu_3 \tau_1 \tan\left[\left(N_2 - \frac{1}{2N_2}\right) k\tau_2\right] \tan(N_3 k\tau_3)$$

$$+i \mu_1 \mu_2^2 N_3 \frac{k\tau_2}{2N_2}$$

$$-i \mu_1^2 \mu_2 \left(N_2 - \frac{1}{2N_2}\right) N_3 \tau_1 \frac{k\tau_2}{2N_2} \tan\left[\left(N_2 - \frac{1}{2N_2}\right) k\tau_2\right]$$

$$+i \mu_1^2 \mu_2 \frac{1}{2N_2} N_3 \tau_1 \qquad (50)$$

$$a_4 = -\mu_2 \mu_3 (N_1^2 - 1) \frac{1}{2N_2} \tau_1 \frac{k\tau_2}{2N_2} \tan\left[\left(N_2 - \frac{1}{2N_2}\right) k\tau_2\right] \tan(N_3 k\tau_3)$$

$$-\mu_2 \mu_3 \left(N_2 - \frac{1}{2N_2}\right) \tau_1 \frac{k\tau_2}{2N_2} \tan\left[\left(N_2 - \frac{1}{2N_2} k\tau_2\right] \tan(N_3 k\tau_3)\right.$$

$$+\mu_2 \mu_3 \frac{1}{2N_2} \tau_1 \tan(N_3 k\tau_3) + \mu_1 \mu_3 \frac{k\tau_2}{2N_2} \tan(N_3 k\tau_3)$$

$$+\mu_2^2 N_3 \tau_1 \frac{k_0 \tau_2}{2N_2} + \mu_1 \mu_2 \frac{1}{2N_2} N_3 \frac{k\tau_2}{2N_2} \tan\left[\left(N_2 - \frac{1}{2N_2}\right) k\tau_2\right] \qquad (51)$$

$$a_5 = -i\mu_1 \mu_2 \mu_3 \frac{1}{2N_2} \tan\frac{k\tau_2}{2N_2} \tan\left[\left(N_2 - \frac{1}{2N_2}\right) k\tau_2\right] \tan(N_3 k\tau_3)$$

$$-i\mu_1^2 \mu_3 \tau_1 \frac{k\tau_2}{2N_2} \tan(N_3 k\tau_3)$$

$$-i\mu_1^2 \mu_2 \frac{1}{2N_2} N_3 \tau_1 \frac{k\tau_2}{2N_2} \tan\left[\left(N_2 - \frac{1}{2N_2}\right) k\tau_2\right] \qquad (52)$$

$$a_6 = -\mu_2 \mu_3 \frac{1}{2N_2} \tau_1 \frac{k_0 \tau_2}{2N_2} \tan\left[\left(N_2 - \frac{1}{2N_2}\right) k\tau_2\right] \tan(N_3 k\tau_3) \qquad (53)$$

A detailed examination of the accuracy of the generalized boundary conditions implied by the constants (40)-(53) as a function of thickness and constitutive parameters is, of course, impractical because of their dependence on numerous geometrical and material parameters. However, guidelines on their accuracy can be drawn from the single layer simulation presented in the previous section.

6. Concluding Remarks

As illustrated in the case of a metal-backed uniform dielectric layer, the generalized boundary conditions (1) provide an excellent simulation of the scattering properties of the structure for thicknesses up to $\lambda/4$ or more for all material properties, directions of incidence and polarizations. For any other structure whose reflection coefficient is known analytically, the appropriate boundary conditions can be derived in a similar manner and their accuracy quantified. Alternatively, if only computed or measured data for the reflection coefficient are available, the required boundary conditions can be found by curve fitting.

For a boundary condition of any given order, the accuracy achieved depends on the location of the surface where the boundary condition is applied, and one advantage of the method we have followed is that the location is treated separately. In the example discussed, the simulating sheet was placed at the upper surface of the dielectric, and a fourth order boundary condition was found to produce excellent results. For other locations, it is necessary to expand the phase factor as indicated in (5), leading to additional derivative factors in the boundary conditions. The optimum location minimizes the complexity of the boundary conditions and/or the error in simulation, and the choice of another location could limit the accuracy achievable. If, in the above application, the simulating sheet was placed at the metal backing, the maximum layer thickness that can be reasonably handled is of order 0.1λ. With the sheet located in this manner, the result of coating the metal is simply to replace the perfectly conducting boundary condition with the appropriate generalized one. It is then only a trivial extension to simulate a metal coated on both sides.

Provided the constants Γ_m and Γ'_m (or a_m and a'_m) satisfy a duality relation (see, for example, (15) or (16)) the boundary condition can be expressed in terms of the tangential field components. This shows that one effect of the higher order derivatives in (1) is to make the boundary conditions less local in character, and the resulting "vector" conditions provide the natural extension of (1) to non-planar surfaces.

In spite of the apparent complication of the generalized boundary conditions and their vector equivalents, it has been found possible to work with them numerically and analytically. Regardless of the order of the conditions, a sheet subject to them supports only tangential electric and magnetic currents. Thus, in a numerical solution of a scattering problem, the number of unknowns is the same as for the standard impedance (first order) boundary condition, and to better simulate coated surfaces, we have already begun to incorporate the higher order conditions into our existing sheet scattering codes employing either the moment or conjugate gradient FFT methods [5,10].

Analytically, it is important to be able to determine the diffraction coefficient for the edge of a half plane or wedge subject to these boundary conditions, and thereby extend the capability of GTD scattering codes. In the case of a half plane we can use either the Maliuzhinets or Wiener-Hopf techniques and [4] is an example of the application of the former, whereas in [11,12] the Wiener-Hopf method was employed. Provided care is taken to ensure that all Fourier transforms exist in the classical sense, the Wiener-Hopf method can handle generalized boundary conditions of any order [13]. The split functions that occur are the same as for a simple impedance boundary condition, with each derivative factor in the boundary condition

giving rise to a pair of split functions. The edge diffraction coefficient then involves a product of these functions.

The proposed boundary conditions have many possible practical applications. In analytical studies of the scattering from junctions and edges, they can be used to model single or multi-layered dielectric slabs or coatings. In numerical treatments, thick coatings can be simulated with a single condition on the surface of the layer, thus, reducing the required number of unknowns at the expense of a slight increase in the complexity of the integral equations. They could also be effective in modelling the dielectric layers used in printed circuit and microstrip arrays, leading to a significant simplification in the Green's functions involved, and we are now examining this possibility.

References

[1] T.B.A. Senior, "Approximate Boundary Conditions," IEEE Trans. Antennas Propagat., vol. AP-29, pp. 826-829, 1981.

[2] T.B.A. Senior, "Impedance Boundary Conditions for Imperfectly Conducting Surfaces," Appl. Sci. Res., vol. 8(B), pp. 418-436, 1960.

[3] A.L. Weinstein, The Theory of Diffraction and the Factorization Method, Golem Press: Boulder, CO., 1969.

[4] J.L. Volakis and T.B.A. Senior, "Applications of a Class of Generalized Boundary Conditions to Scattering by a Metal-Backed Dielectric Half-Plane," Proc. IEEE, May 1989.

[5] T.B.A. Senior and J.L. Volakis, "Sheet Simulation of a Thin Dielectric Layer," Radio Sci., vol. 22, pp. 1261-1272, 1987.

[6] B. Engquist and A. Majda, "Absorbing Boundary Conditions for the Numerical Simulation of Waves," Math. Comput., vol. 31, pp. 629-651, 1977.

[7] L. N. Trefethen and L. Halpern, "Well-Posedness of One-Way Equations and Absorbing Boundary Conditions," Math. Comp., vol. 47, pp. 421-435, 1986.

[8] S.N. Karp and F.C. Karal, Jr., "Generalized Impedance Boundary Conditions with Applications to Surface Wave Structures," in Electromagnetic Wave Theory, Part 1, ed. J. Brown, pp. 479-483, Pergamon: New York, 1965.

[9] T.B.A. Senior, "Some Problems Involving Imperfect Half-Planes," in Electromagnetic Scattering, ed. P.L.E. Uslenghi, pp. 185-219, Academic Press: New York, 1978.

[10] M.A. Ricoy and J.L. Volakis, "Integral Equations with Reduced Unknowns for the Simulation of Two-Dimensional Composite Structures," IEEE Trans. Antennas Propagat., March 1989 (in press).

[11] J.L. Volakis and T.B.A. Senior, "Diffraction by a Thin Dielectric Half Plane," IEEE Trans. Antennas Propagat., AP-35, pp. 1483-1487, 1987.

[12] J.L. Volakis, "High Frequency Scattering by a Material Half-Plane and Strip," Radio Sci., 23, pp. 450-462, May-June 1988.

[13] T.B.A. Senior, "A Critique of Certain Half-Plane Diffraction Analyses," Electromagnetics, vol. 7, pp. 81-90, 1987.

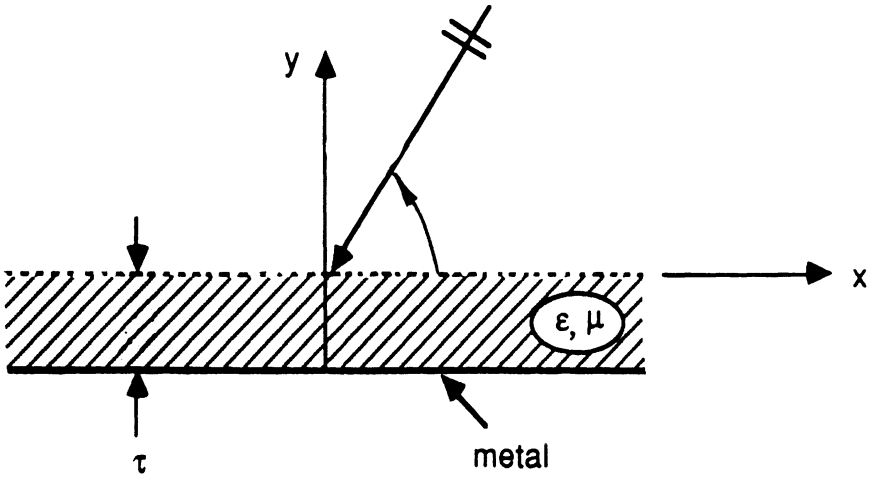

Figure 1

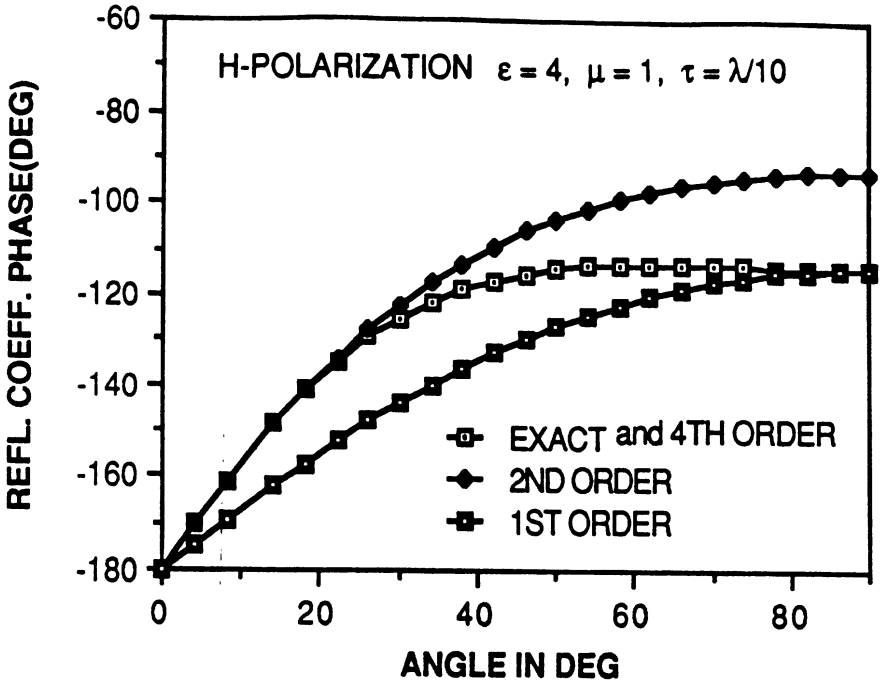
H-POLARIZATION ε = 4, μ = 1, τ = λ/10
REFL. COEFF. PHASE(DEG)
-60
-80
-100
-120
-140
-160
-180
0
20
40
60
80
ANGLE IN DEG
EXACT and 4TH ORDER
2ND ORDER
1ST ORDER

(a)

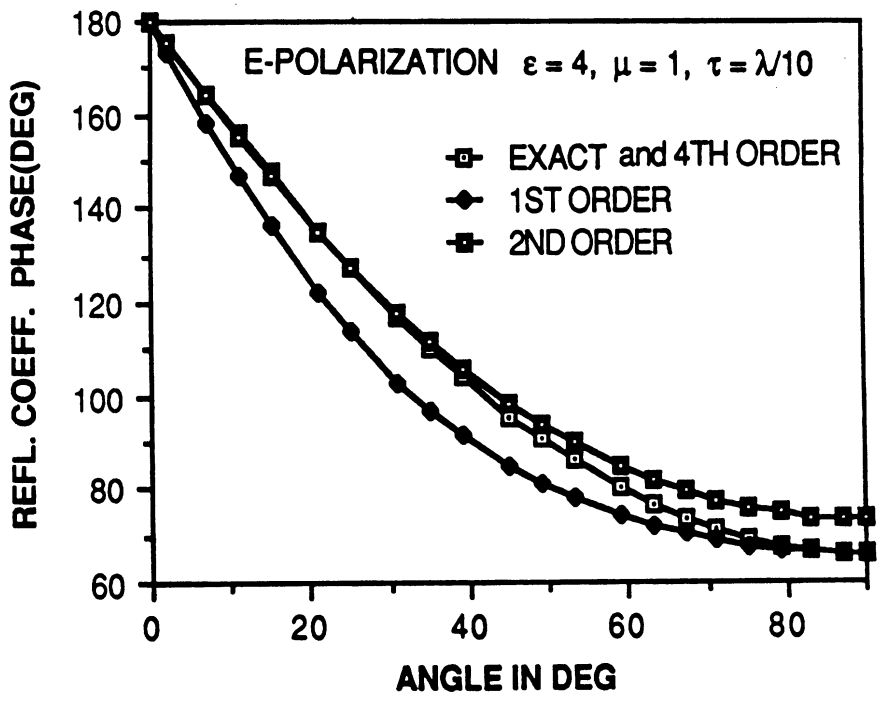
E-POLARIZATION ε = 4, μ = 1, τ = λ/10
REFL. COEFF. PHASE(DEG)
180
160
140
120
100
80
60
0
20
40
60
80
ANGLE IN DEG
EXACT and 4TH ORDER
1ST ORDER
2ND ORDER

(b)

Figure 2

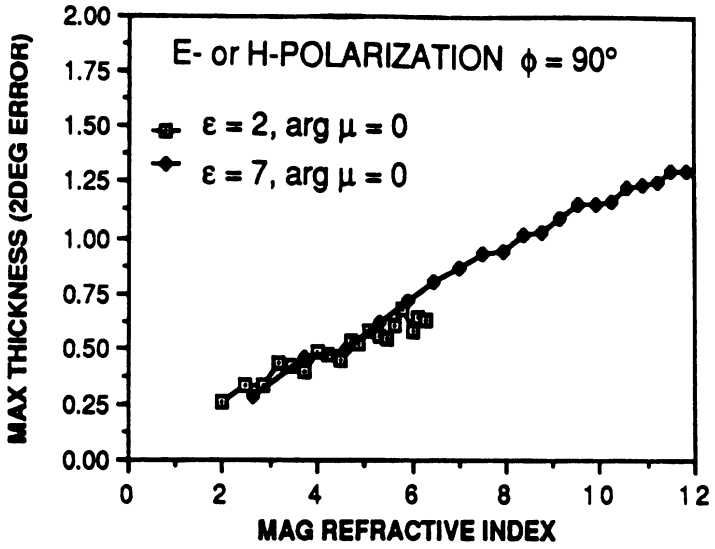
E- or H-POLARIZATION ϕ = 90°
ε = 2, arg μ = 0
ε = 7, arg μ = 0
MAX THICKNESS (2DEG ERROR)
MAG REFRACTIVE INDEX
2.00
1.75
1.50
1.25
1.00
0.75
0.50
0.25
0.00
0
2
4
6
8
10
12

Figure 3

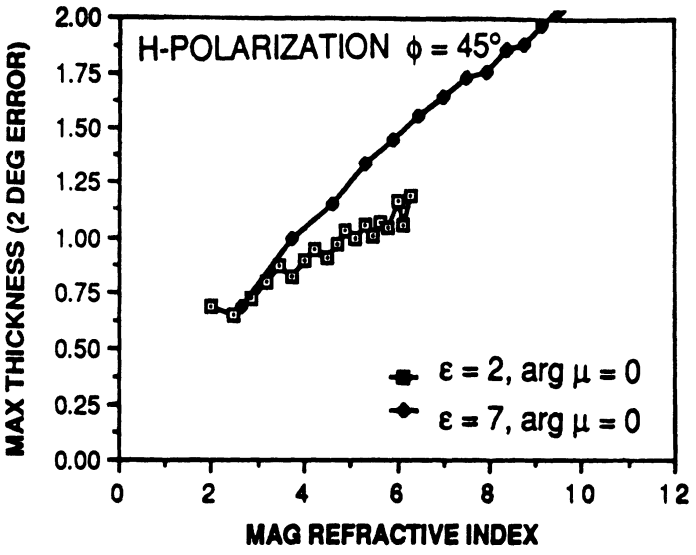
H-POLARIZATION ϕ = 45°
MAX THICKNESS (2 DEG ERROR)
MAG REFRACTIVE INDEX
ε = 2, arg μ = 0
ε = 7, arg μ = 0
2.00
1.75
1.50
1.25
1.00
0.75
0.50
0.25
0.00
0
2
4
6
8
10
12

(a)

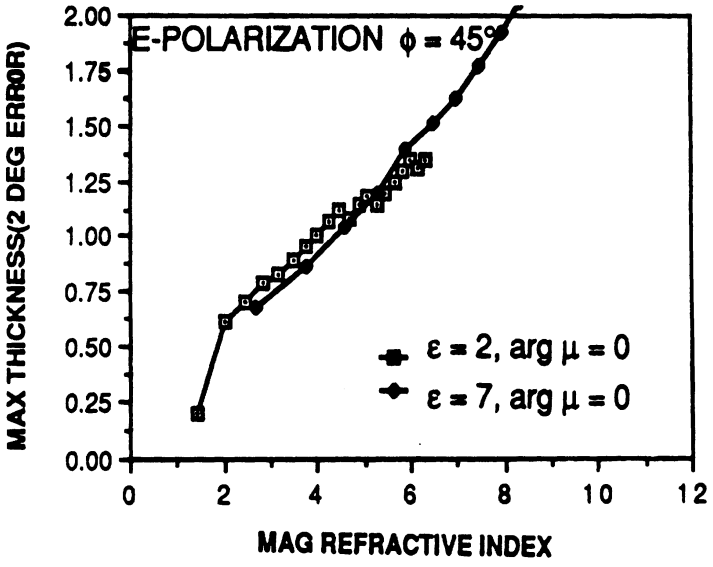
E-POLARIZATION ϕ = 45°
MAX THICKNESS(2 DEG ERROR)
MAG REFRACTIVE INDEX
ε = 2, arg μ = 0
ε = 7, arg μ = 0
2.00
1.75
1.50
1.25
1.00
0.75
0.50
0.25
0.00
0
2
4
6
8
10
12

(b)

Figure 4

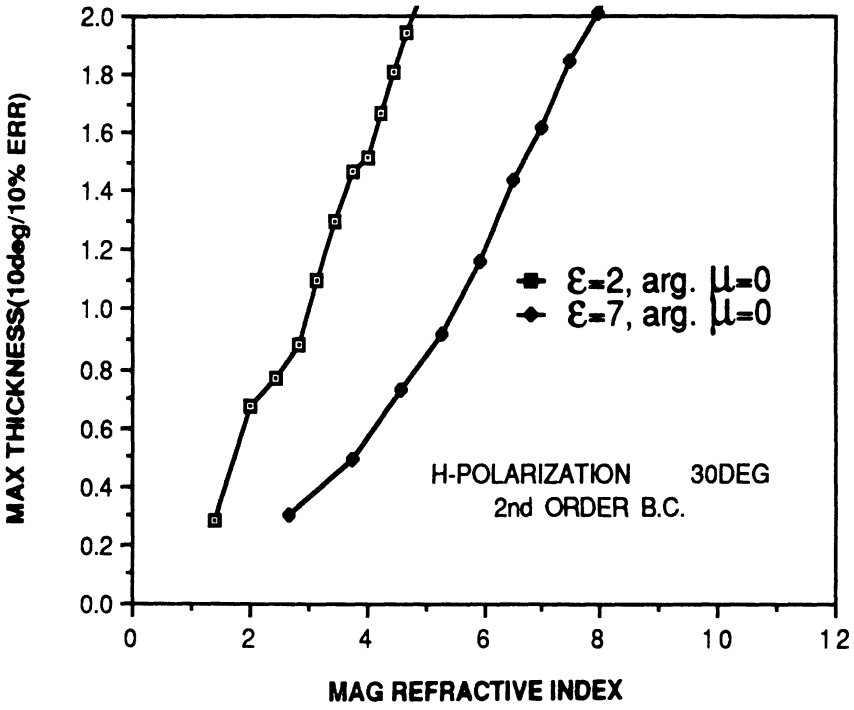
MAX THICKNESS(10deg/10% ERR)
2.0
1.8
1.6
1.4
1.2
1.0
0.8
0.6
0.4
0.2
0.0
0
2
4
6
8
10
12
MAG REFRACTIVE INDEX
ε=2, arg. μ=0
ε=7, arg. μ=0
H-POLARIZATION 30DEG
2nd ORDER B.C.

(a)

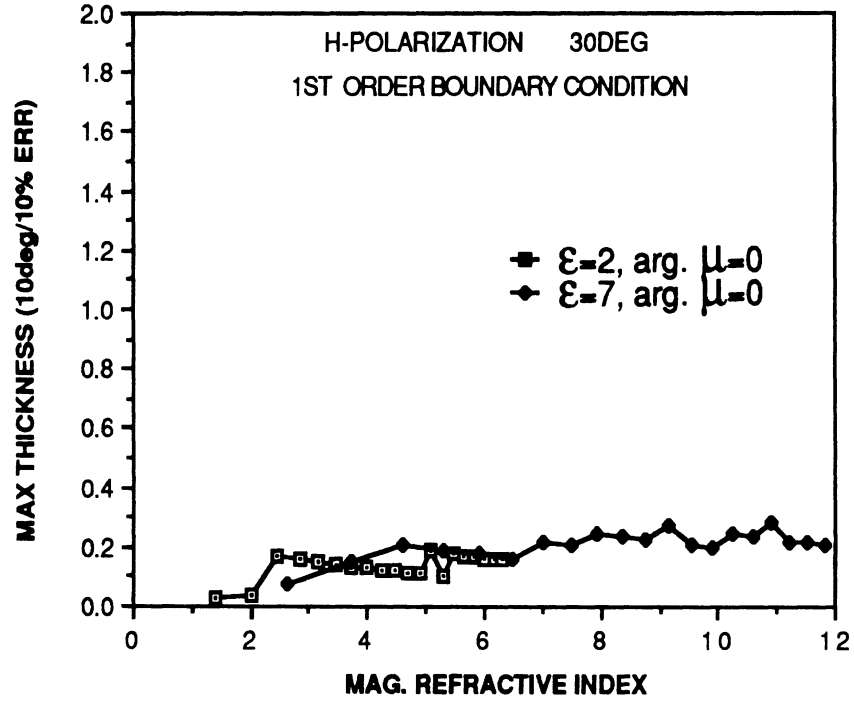
MAX THICKNESS (10deg/10% ERR)
2.0
1.8
1.6
1.4
1.2
1.0
0.8
0.6
0.4
0.2
0.0
0
2
4
6
8
10
12
MAG. REFRACTIVE INDEX
H-POLARIZATION 30DEG
1ST ORDER BOUNDARY CONDITION
ε=2, arg. μ=0
ε=7, arg. μ=0

(b)

Figure 5

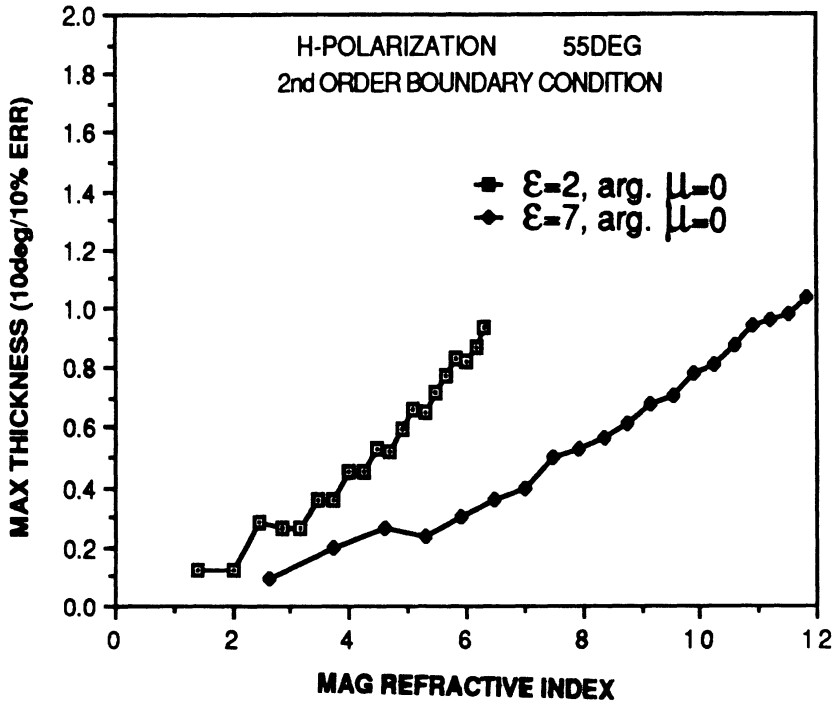
H-POLARIZATION 55DEG
2nd ORDER BOUNDARY CONDITION
ε=2, arg. μ=0
ε=7, arg. μ=0
MAX THICKNESS (10deg/10% ERR)
MAG REFRACTIVE INDEX
0.0
0.2
0.4
0.6
0.8
1.0
1.2
1.4
1.6
1.8
2.0
0
2
4
6
8
10
12

(a)

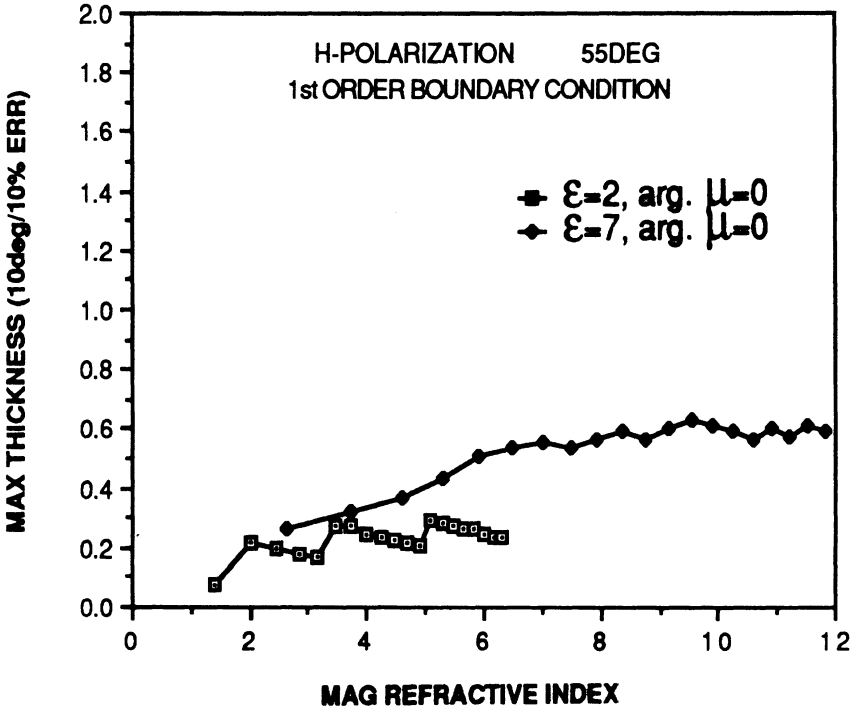
H-POLARIZATION 55DEG
1st ORDER BOUNDARY CONDITION
ε=2, arg. μ=0
ε=7, arg. μ=0
MAX THICKNESS (10deg/10% ERR)
MAG REFRACTIVE INDEX
0.0
0.2
0.4
0.6
0.8
1.0
1.2
1.4
1.6
1.8
2.0
0
2
4
6
8
10
12

(b)

Figure 6

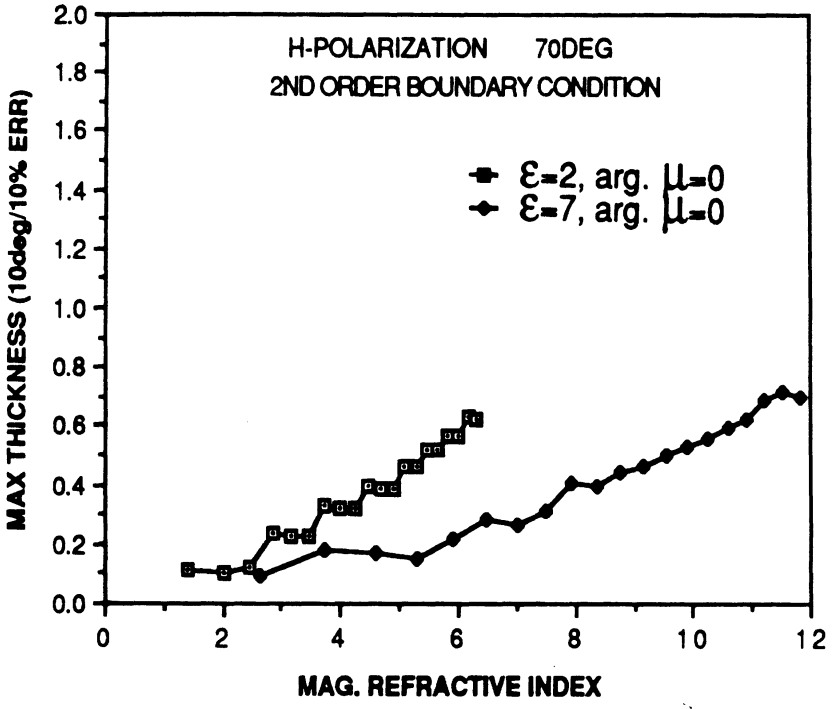
H-POLARIZATION 70DEG
2ND ORDER BOUNDARY CONDITION
ε=2, arg. μ=0
ε=7, arg. μ=0
MAX THICKNESS (10deg/10% ERR)
MAG. REFRACTIVE INDEX
0.0
0.2
0.4
0.6
0.8
1.0
1.2
1.4
1.6
1.8
2.0
0
2
4
6
8
10
12

(a)

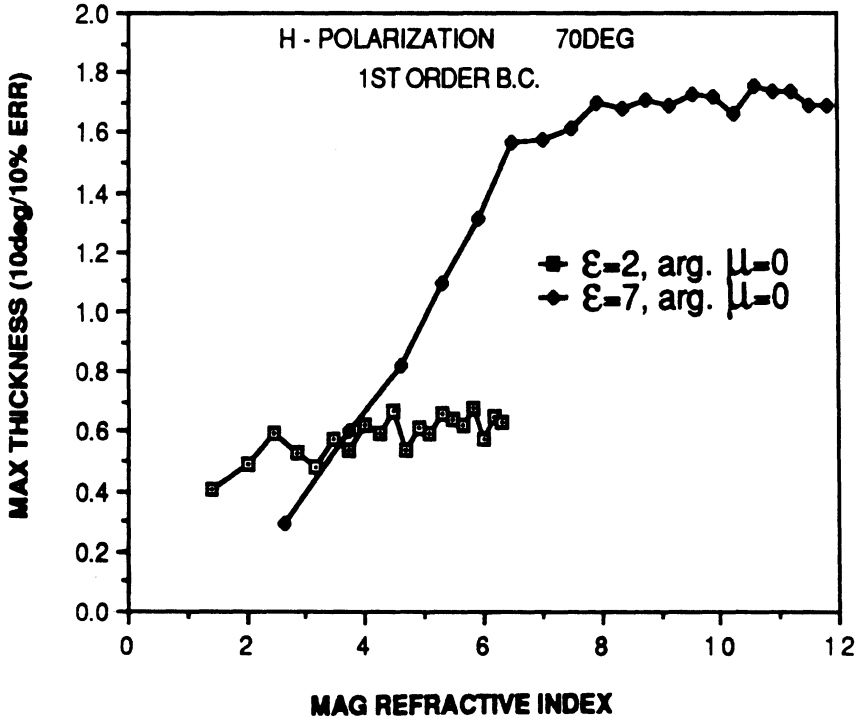
H - POLARIZATION 70DEG
1ST ORDER B.C.
ε=2, arg. μ=0
ε=7, arg. μ=0
MAX THICKNESS (10deg/10% ERR)
MAG REFRACTIVE INDEX
0.0
0.2
0.4
0.6
0.8
1.0
1.2
1.4
1.6
1.8
2.0
0
2
4
6
8
10
12

(b)

Figure 7

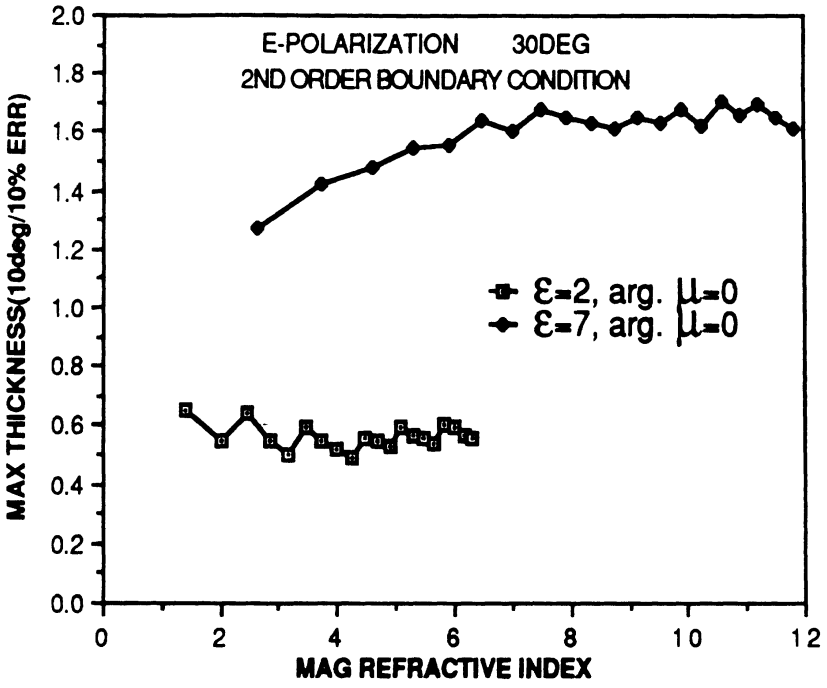
E-POLARIZATION 30DEG
2ND ORDER BOUNDARY CONDITION
ε=2, arg. μ=0
ε=7, arg. μ=0
MAX THICKNESS(10deg/10% ERR)
MAG REFRACTIVE INDEX
0.0
0.2
0.4
0.6
0.8
1.0
1.2
1.4
1.6
1.8
2.0
0
2
4
6
8
10
12

(a)

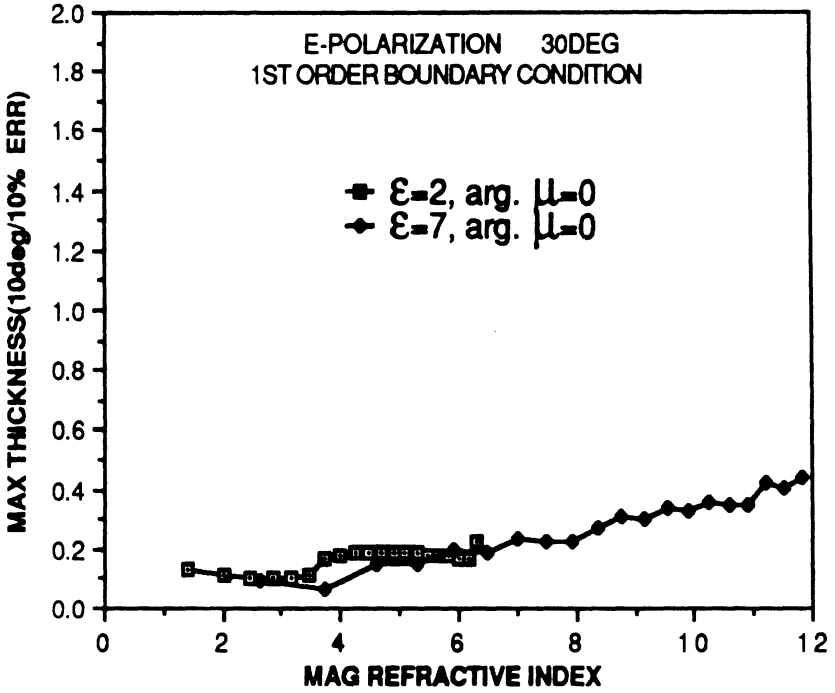
E-POLARIZATION 30DEG
1ST ORDER BOUNDARY CONDITION
ε=2, arg. μ=0
ε=7, arg. μ=0
MAX THICKNESS(10deg/10% ERR)
MAG REFRACTIVE INDEX
0.0
0.2
0.4
0.6
0.8
1.0
1.2
1.4
1.6
1.8
2.0
0
2
4
6
8
10
12

(b)

Figure 8

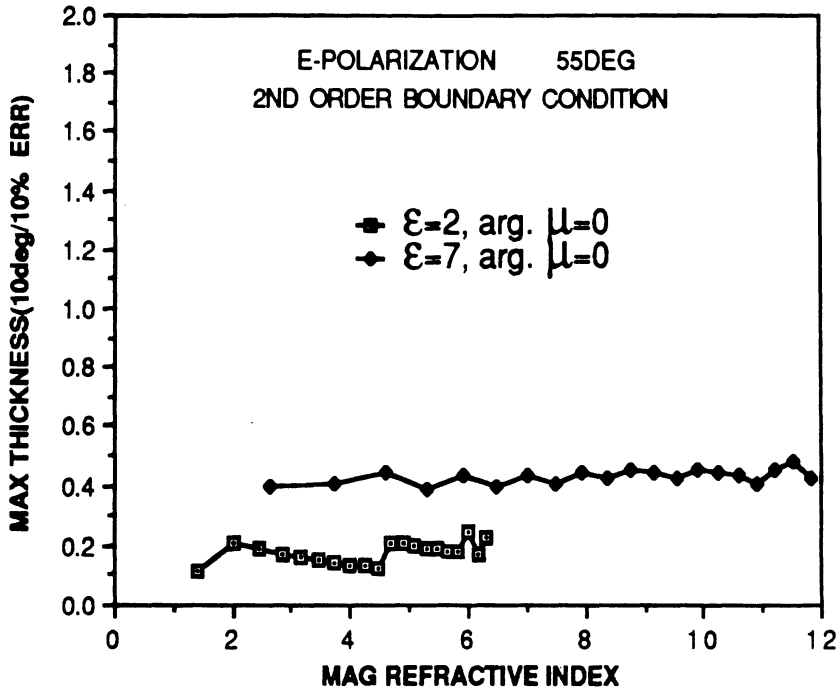
E-POLARIZATION 55DEG
2ND ORDER BOUNDARY CONDITION
ε=2, arg. μ=0
ε=7, arg. μ=0
MAX THICKNESS(10deg/10% ERR)
MAG REFRACTIVE INDEX
0.0
0.2
0.4
0.6
0.8
1.0
1.2
1.4
1.6
1.8
2.0
0
2
4
6
8
10
12

(a)

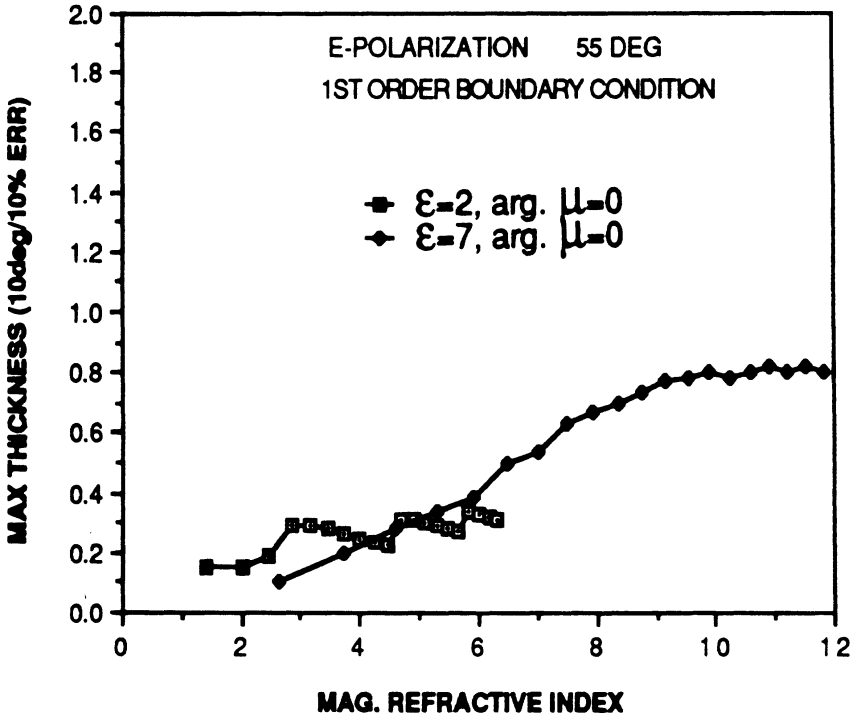
E-POLARIZATION 55 DEG
1ST ORDER BOUNDARY CONDITION
ε=2, arg. μ=0
ε=7, arg. μ=0
MAX THICKNESS (10deg/10% ERR)
MAG. REFRACTIVE INDEX
0.0
0.2
0.4
0.6
0.8
1.0
1.2
1.4
1.6
1.8
2.0
0
2
4
6
8
10
12

(b)

Figure 9

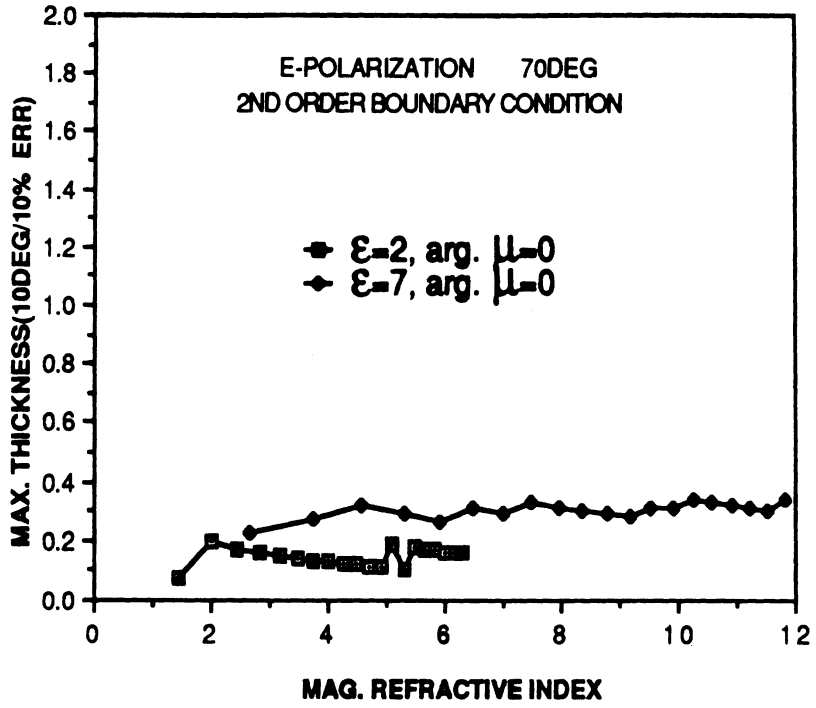
E-POLARIZATION 70DEG
2ND ORDER BOUNDARY CONDITION
ε=2, arg. μ=0
ε=7, arg. μ=0
MAX. THICKNESS(10DEG/10% ERR)
MAG. REFRACTIVE INDEX
0.0
0.2
0.4
0.6
0.8
1.0
1.2
1.4
1.6
1.8
2.0
0
2
4
6
8
10
12

(a)

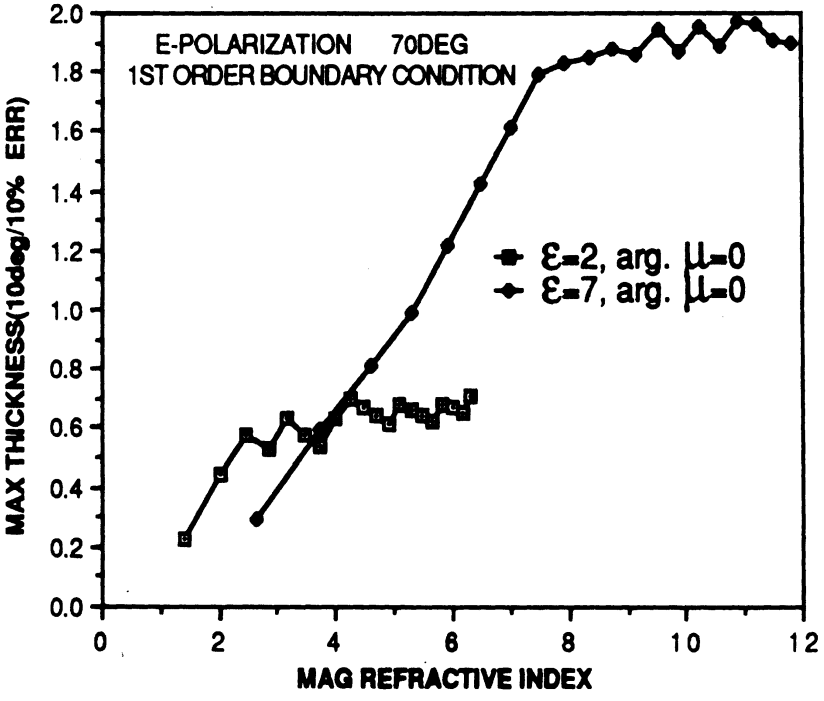
E-POLARIZATION 70DEG
1ST ORDER BOUNDARY CONDITION
ε=2, arg. μ=0
ε=7, arg. μ=0
MAX THICKNESS(10deg/10% ERR)
MAG REFRACTIVE INDEX
0.0
0.2
0.4
0.6
0.8
1.0
1.2
1.4
1.6
1.8
2.0
0
2
4
6
8
10
12

(b)

Figure 10

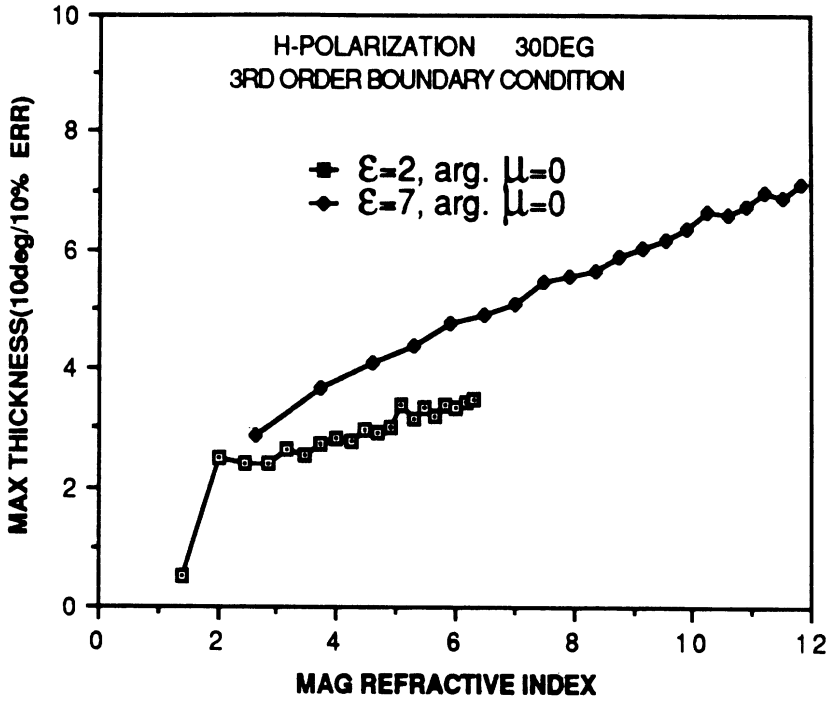
H-POLARIZATION 30DEG
3RD ORDER BOUNDARY CONDITION
ε=2, arg. μ=0
ε=7, arg. μ=0
MAX THICKNESS(10deg/10% ERR)
MAG REFRACTIVE INDEX
0
2
4
6
8
10
12

(a)

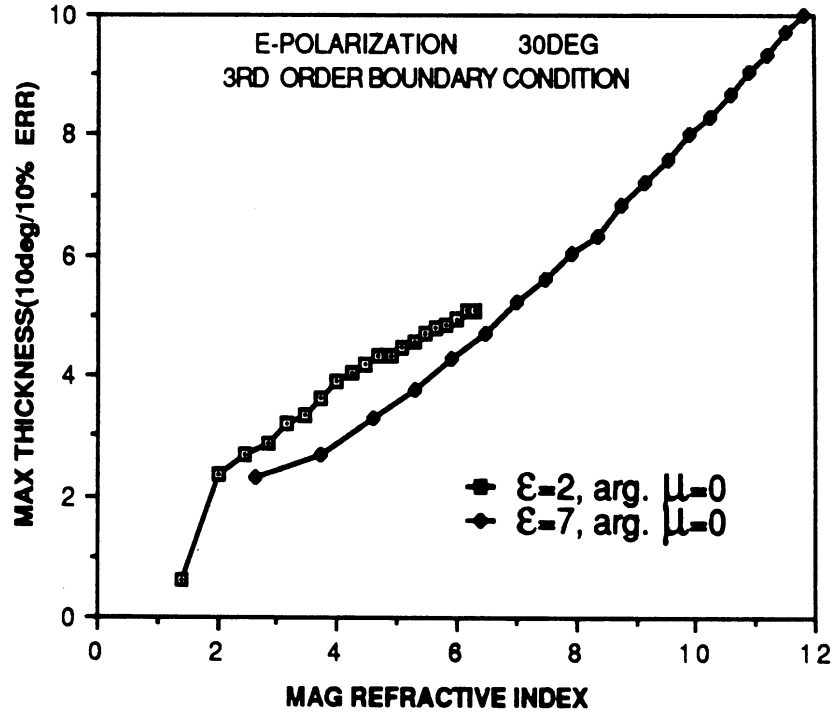
E-POLARIZATION 30DEG
3RD ORDER BOUNDARY CONDITION
ε=2, arg. μ=0
ε=7, arg. μ=0
MAX THICKNESS(10deg/10% ERR)
MAG REFRACTIVE INDEX
0
2
4
6
8
10
12

(b)

Figure 11

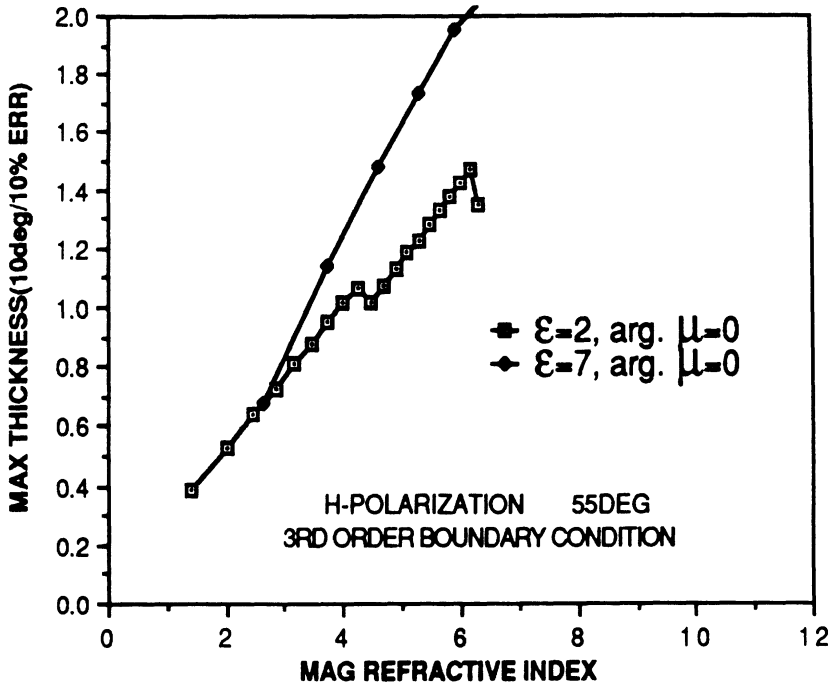
MAX THICKNESS(10deg/10% ERR)
2.0
1.8
1.6
1.4
1.2
1.0
0.8
0.6
0.4
0.2
0.0
0
2
4
6
8
10
12
MAG REFRACTIVE INDEX
ε=2, arg. μ=0
ε=7, arg. μ=0
H-POLARIZATION 55DEG
3RD ORDER BOUNDARY CONDITION

(a)

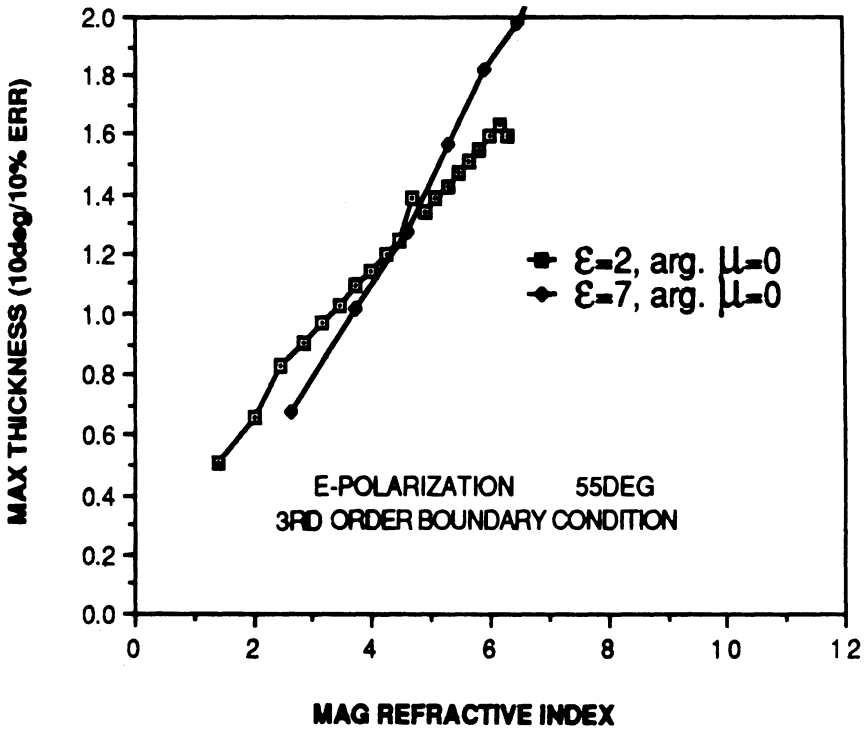
MAX THICKNESS (10deg/10% ERR)
2.0
1.8
1.6
1.4
1.2
1.0
0.8
0.6
0.4
0.2
0.0
0
2
4
6
8
10
12
MAG REFRACTIVE INDEX
ε=2, arg. μ=0
ε=7, arg. μ=0
E-POLARIZATION 55DEG
3RD ORDER BOUNDARY CONDITION

(b)

Figure 12

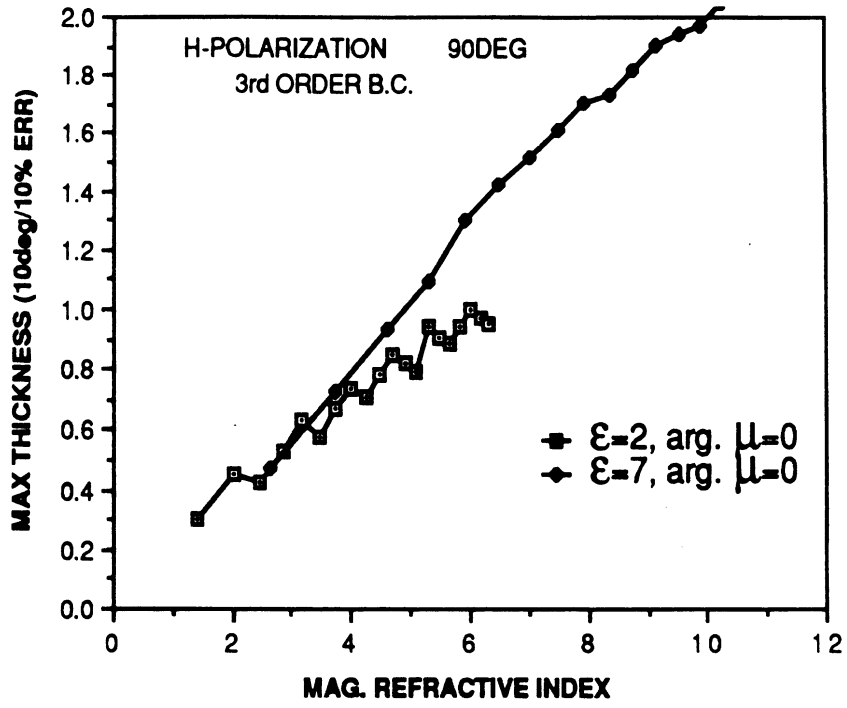
H-POLARIZATION 90DEG
3rd ORDER B.C.
MAX THICKNESS (10deg/10% ERR)
MAG. REFRACTIVE INDEX
ε=2, arg. μ=0
ε=7, arg. μ=0
0.0
0.2
0.4
0.6
0.8
1.0
1.2
1.4
1.6
1.8
2.0
0
2
4
6
8
10
12

(a)

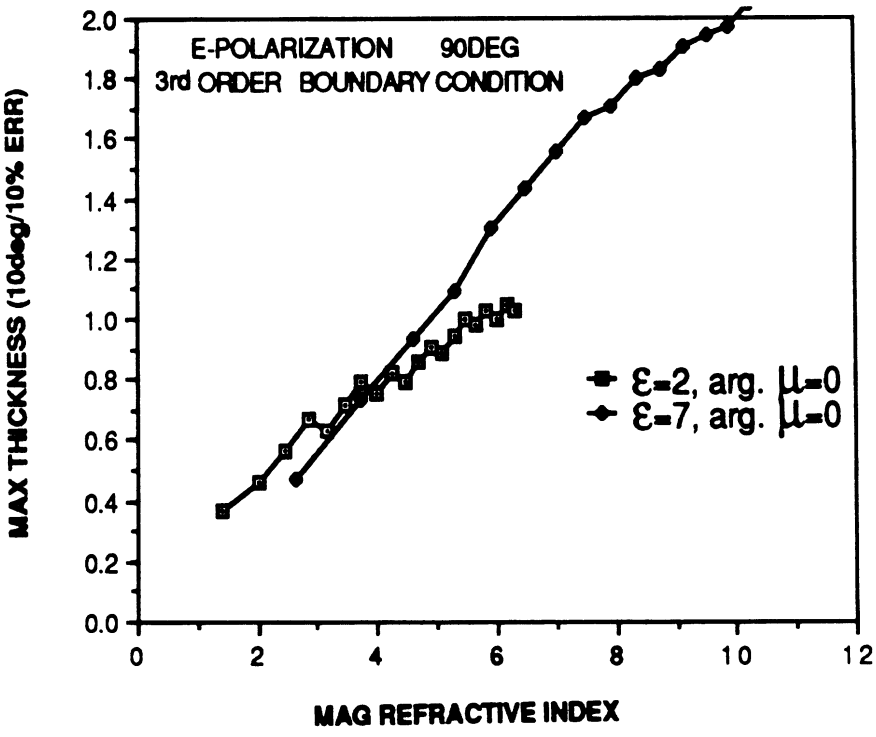
E-POLARIZATION 90DEG
3rd ORDER BOUNDARY CONDITION
MAX THICKNESS (10deg/10% ERR)
MAG REFRACTIVE INDEX
ε=2, arg. μ=0
ε=7, arg. μ=0
0.0
0.2
0.4
0.6
0.8
1.0
1.2
1.4
1.6
1.8
2.0
0
2
4
6
8
10
12

(b)

Figure 13

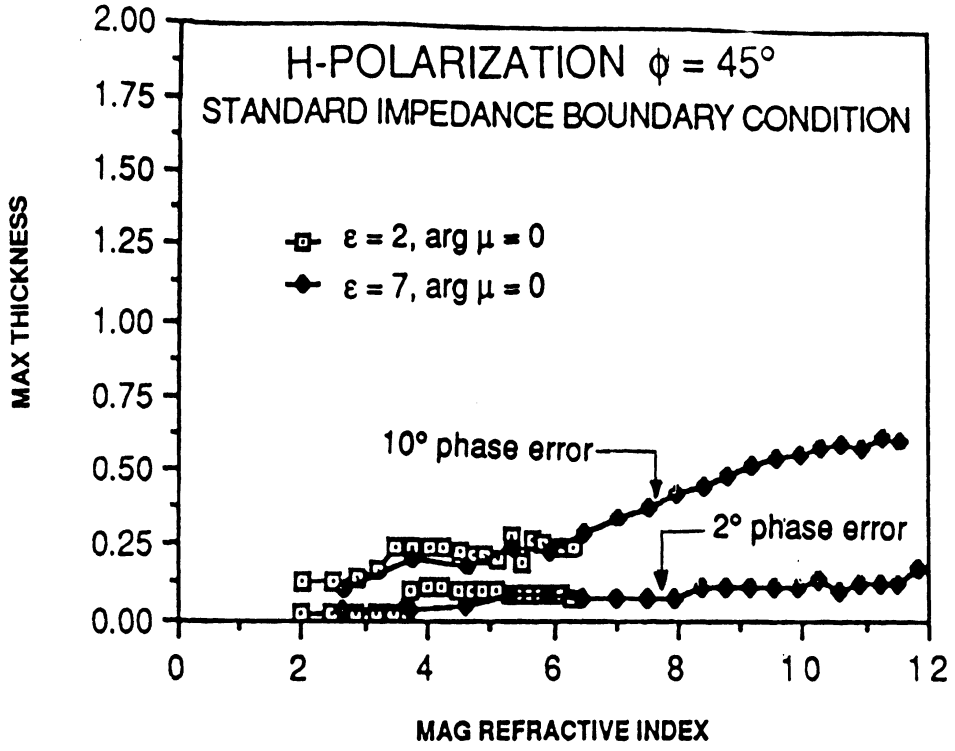
H-POLARIZATION ϕ = 45°
STANDARD IMPEDANCE BOUNDARY CONDITION
ε = 2, arg μ = 0
ε = 7, arg μ = 0
10° phase error
2° phase error
MAX THICKNESS
MAG REFRACTIVE INDEX
2.00
1.75
1.50
1.25
1.00
0.75
0.50
0.25
0.00
0
2
4
6
8
10
12

(a)

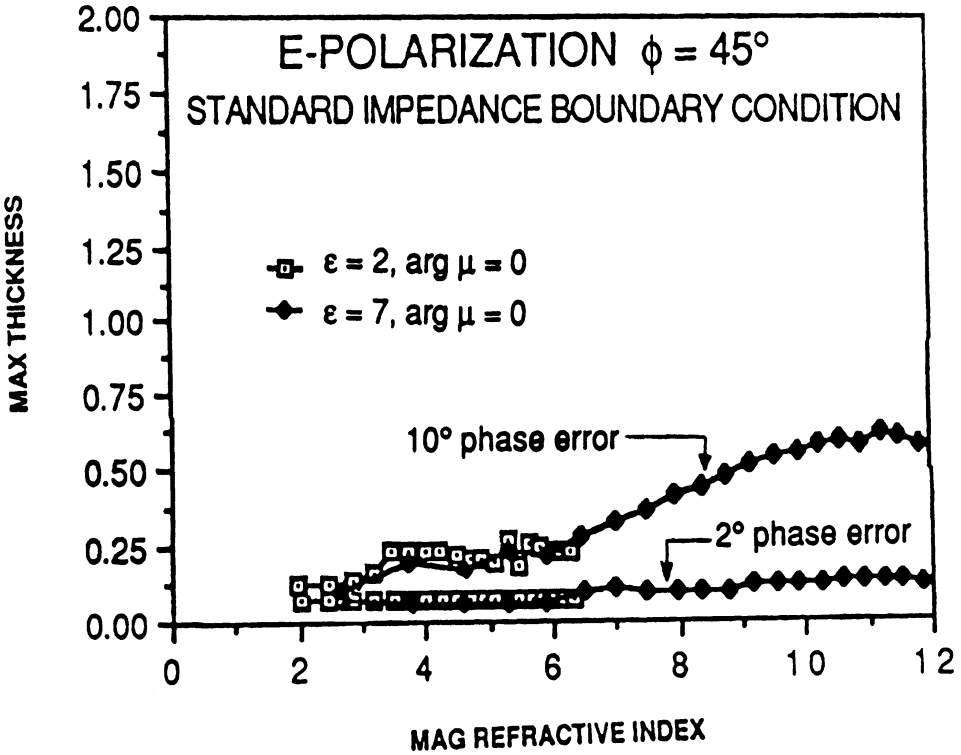
E-POLARIZATION ϕ = 45°
STANDARD IMPEDANCE BOUNDARY CONDITION
ε = 2, arg μ = 0
ε = 7, arg μ = 0
10° phase error
2° phase error
MAX THICKNESS
MAG REFRACTIVE INDEX
2.00
1.75
1.50
1.25
1.00
0.75
0.50
0.25
0.00
0
2
4
6
8
10
12

(b)

Figure 14

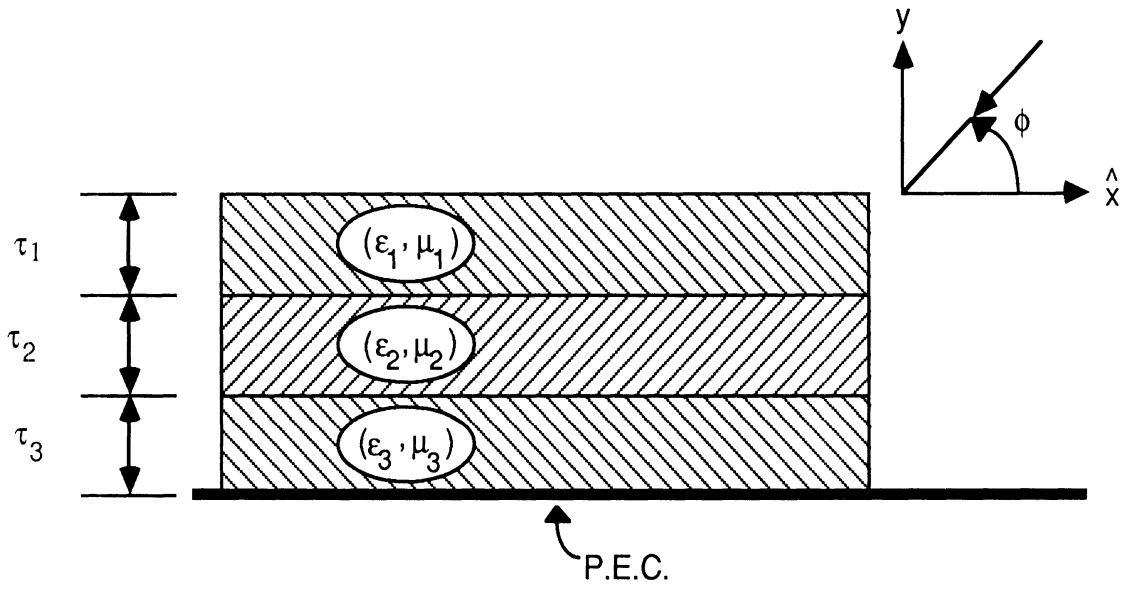

FIGURE 15